Masters Program in Geospatial Technologies

ANALYSIS OF TEMPORAL AND SPATIAL VARIATION OF FOREST

A case of study in northeastern Armenia

Gohar Ghazaryan

Dissertation submitted in partial fulfilment of the requirements
for the Degree of *Master of Science in Geospatial Technologies*

UNIVERSIDADE NOVA ISEGI
UNIVERSITAT JAUME·I
WESTFÄLISCHE WILHELMS-UNIVERSITÄT MÜNSTER

ANALYSIS OF TEMPORAL AND SPATIAL VARIATION OF FOREST

A case of study in northeastern Armenia

Dissertation supervised by

Supervisor:
Prof. Dr. Edzer Pebesma, Institute for Geoinformatics, University of Muenster

Co-supervisors:
Prof. Mark Padgham, Institute for Geoinformatics, University of Muenster

Prof. Filiberto Pla, Institute of New Imaging Technologies University Jaume I

February, 2015

DECLERATION OF ORIGINALITY

The following Master thesis was prepared in my own words without any additional help. All used sources of literature are listed at the end of the thesis.

The thesis was not submitted in the same or in a similar version to achieve an academic grading.

Muenster, 26.02.2015 Gohar Ghazaryan

ACKNOWLEDGMENTS

I appreciate my supervisor Prof. Dr. Edzer Pebesma for the great support, guidance and constructive comments. Also I would like to thank co-supervisors Prof. Mark Padgham and Prof. Filiberto Pla for their time spent on my thesis.

I want to thank Ms. Ana Sousa, Prof. Dr. Marco Pinho, Prof. Brox and to every member of staff at ifgi and UNL for my wonderful study experience.

I can't thank enough GEE developers and especially Ian Hausman for continuous support and assistance.

I would especially like to thank Prof. Samvel Nahapetyan and Prof. Hovik Sayadyan for their help and encouragement.

Last but not the least I would like to thank my family and friends for encouragement, support and love that I got.

ANALYSIS OF TEMPORAL AND SPATIAL VARIATION OF FOREST

A case of study in northeastern Armenia

ABSTRACT

The forest has a crucial ecological role and the continuous forest loss can cause colossal effects on the environment. As Armenia is one of the low forest covered countries in the world, this problem is more critical. Continuous forest disturbances mainly caused by illegal logging started from the early 1990s had a huge damage on the forest ecosystem by decreasing the forest productivity and making more areas vulnerable to erosion. Another aspect of the Armenian forest is the lack of continuous monitoring and absence of accurate estimation of the level of cuts in some years.

In order to have insight about the forest and the disturbances in the long period of time we used Landsat TM/ETM + images. Google Earth Engine JavaScript API was used, which is an online tool enabling the access and analysis of a great amount of satellite imagery.

To overcome the data availability problem caused by the gap in the Landsat series in 1988-1998, extensive cloud cover in the study area and the missing scan lines, we used pixel based compositing for the temporal window of leaf on vegetation (June-late September). Subsequently, pixel based linear regression analyses were performed.

Vegetation indices derived from the 10 biannual composites for the years 1984-2014 were used for trend analysis.

In order to derive the disturbances only in forests, forest cover layer was aggregated and the original composites were masked. It has been found, that around 23% of forests were disturbed during the study period.

TABLE OF CONTENT

KEYWORDS

Forest

Forest disturbances

Trend analysis

Pixel based regressions

Google Earth Engine

ACRONYMS

GEE – Google Earth Engine

TM – Thematic mapper

ETM+ – Enhanced thematic mapper

VI– Vegetation index

NIR – Near Infrared

SWIR – Short Wave Infrared

NDVI – Normalized Difference Vegetation Index

NDMI – Normalized Difference Moisture Index

ATP – Armenian tree project

FAO – Food and Agriculture Organization of the United Nations

OLS – Ordinary least squares

INDEX OF TABLES

INDEX OF FIGURES

CHAPTER ONE
INTRODUCTION

1.1 Theoretical Framework

Deforestation and forest degradation are one of the biggest environmental problems and their impact can be colossal. Forests, the most complex terrestrial ecosystems on the earth, have an important ecological role in the conservation of biological diversity, they store a vast amount of carbon, prevent soil erosion.

Forest cover changes, especially those of anthropogenic origin, have broad impacts on critical environmental processes including Earth's energy balance, water cycle, and biogeochemical processes. Quantifying such changes is required for addressing many pressing issues including the global carbon budget, ecosystem dynamics, sustainability, and the vulnerability of natural and human systems (Huang et al., 2008).

Scientists and policy makers from various institutions and agencies are currently devoting substantial time and resources to study the implications of the environmental change in forests and woodlands, the most widely distributed ecosystem on earth (Rogan et al., 2006). Forests provide key ecological goods and services for many other plants and animals, as well as for humans (Weng, 2011). Consequently, the reduction of the forested area can have dramatic outcomes. Although the rate of deforestation shows signs of decreasing, it is still alarmingly high. It shows signs of decreasing in several countries but continues at a high rate in others (FAO, 2010).

In general, deforestation has been attributed to socio-demographic factors, such as population growth, economy and specific exploitation activities like commercial logging, forest farming, fuel wood gathering, and pasture clearance for cattle production (FAO, 2007).

The current state of deforestation is critical in Armenia as well. The Armenian forests are under the highest socioeconomic pressures, threat of degradation or destruction (Moreno-Sanchez et al., 2007). This is due to uncontrolled forest logging, which was at its peak starting from early 1990s. As reported by the Armenian tree project, Armenia is facing one of the worst ecological threats. In fact, over 750,000 cubic meters of forest coverage are now being cut annually. At the current rate of deforestation, Armenia faces the probability of turning into a barren desert within 50 years (Armenian tree project, 2013). Hergnyan et al., (2006) stated that Armenia is one of the 70 low forest-covered countries, as the forests cover

is less than 10% of the total land area. Hence, the continuing deforestation of forest resources presents a significant environmental threat combined with destroying consequences for habitats, irreversible losses of biodiversity, lost revenue of the government from the alternative benefits of the forest (e.g. tourism development). The economic crisis and the drastic socio-economic conditions, along with the poor implementation of forest management and monitoring policies throughout the 1990s have resulted in massive deforestation of the country. Due to the strengthened state control during the recent years the logging volumes have decreased. However, the overall decrease of the forest resources is still progressing, despite the major efforts of international and local organizations towards intensive reforestation. Taking into account economic, social and political conditions in the country, Moreno-Sanchez et al., (2005) predict that the decline of the forest will continue and it will probably accelerate.

Because of absence of continuous forest monitoring in the study area, there is a need of studies which will reveal the current state of forest ecosystems, rate of deforestation, disturbances during long period and it can give essential contribution in decision making for sustainable use of forest. To achieve this aim, remotely sensed data can be used.

Remote Sensing provides a unique opportunity to assess and monitor deforestation, degradation, and fragmentation for a number of reasons. First, it allows detailed study from local level to global forest resources assessment. Furthermore, remotely sensed data can be acquired repeatedly (e.g. daily, monthly), which helps to monitor forest resources in a regular basis (FAO, 2007). Both the gradual changes of forest succession and the sudden change of deforestation due to anthropogenic (e.g., timber harvesting) or natural (e.g., fire) disturbances can be detected by satellite imagery. It is usually quite straightforward to map deforestation with Landsat TM/ETM+ imagery as a result of dramatic change in surface reflectance before and after the disturbance (Weng 2011).

The increasing availability of satellite imagery with different spatial, spectral and temporal characteristics and the development of data analysis methods give a chance for having better idea about forest change patterns. In several studies the potential of detecting changes within time series is shown, which benefits from temporal depth of satellite imagery and gives an idea about trends of changes.

1.2 Statement of the Problem

The last few decades have seen a reduction of the extent and quality of the forest cover in Armenia. Years of unsustainable and illegal logging have reduced both forest quantity and quality. Following the independence, an energy crisis led to significant deforestation, reducing Armenia's already minimal forest cover.

The decade of the 1990s was harsh and turbulent in Armenia. In 1991 Armenia got its independence from the former USSR. During the following year the country experienced political violence and several economic shocks. The separation from the USSR, compounded by a devastating earthquake in 1988, and the 1988-1994 war with the neighboring Republic of Azerbaijan created a transportation, economic and energy blockade. This situation put a tremendous pressure on the forests as source of fuel wood. It is estimated that during the 1990s nearly 50% of the energy consumed in households near to forested areas came from fuel wood. As a result, the most valuable species of trees were logged (Thuresson et al., 1999; Moreno-Sanchez et al., 2005; Junge & Fripp 2011).

There is no accurate estimation of the level of cuts during that period and the estimations are different from author to author. More trustful information about forest logging is available from late 1990s. Another threat for forest is the copper mining, which occupies large forested areas in northeastern Armenia.

Figure 1 illustrates the volume of cuts from 1999 till nowadays. The values are aggregated from different sources (Moreno-Sanchez et al., 2005; Hergnyan et al., 2006; Hayantar 2014), and they approximate the available data. Although, the economic conditions in the country have been improved, the volume of cuts remained high for a few years and slowly has been stabilizing in recent years.

Although there were some studies on forest degradation in Armenia, only few of them have used geospatial technologies to reveal forest disturbance level. One of the latest studies in the north-eastern area of Armenia shows the change in forest cover in the study area and estimates the change from ~25% in 1989 to ~19% in the year 2000 (Asiryan, 2005).

The understanding of seriousness of this problem and the lack of research aiming to detect the deforestation and the forest degradation and making further analysis were the main motivation to do this thesis research. Furthermore, the existing studies focus on spatial change and depict the change from 2 time steps. In this thesis study not only the spatial changes of the forest are discussed, but also the temporal context of change is considered.

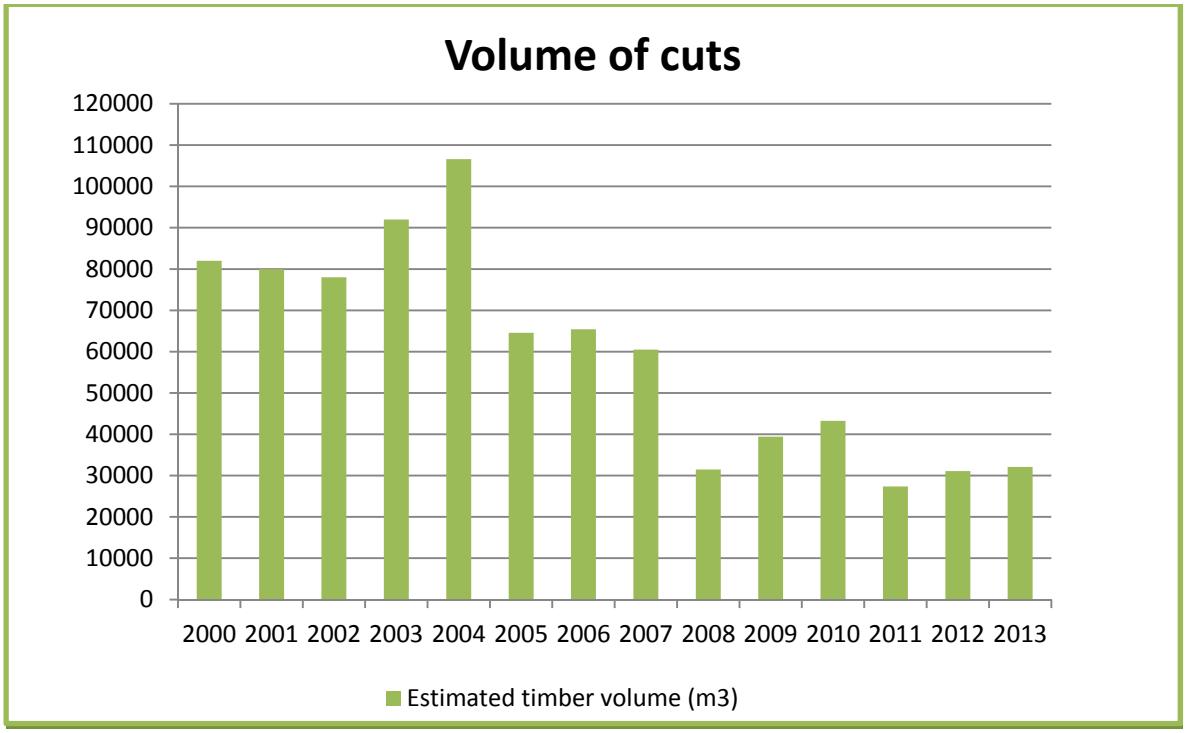

Figure 1: The volume of forest logging in Armenia derived from available sources

Moreno-Sanchez et al., (2005); Hergnyan et al., (2006); Hayantar (2014)

1.3 Study Area at glance

The study area is located in the north-eastern part of Armenia. The area comprises the biggest forested areas in Armenia. At the same time this area is described as one of the most vulnerable areas to deforestation and forest degradation.

The main deforestation threats are fuel wood gathering, infrastructure and mining. Deforestation in this area is expressed as clear cuts around the large cities. Another major feature of deforestation process is the accelerated rates of forest fragmentation. The increasingly complex shapes of large forest patches distort the forestry estimates: the forest degradation continues leaving the surface of forest cover relatively unchanged (Hergnyan et al., 2006). In addition to anthropogenic disturbances, large areas of forests are destroyed by natural causes: wind, erosion and landslides, forest fires. Large areas of forest disturbances caused by wind were reported in 2004 and 2007 (Hayantar, 2014). Figure 2 illustrates wind fallen trees in 2007.

The study area is characterized by strong topography. Its regular cloud cover poses a challenge for studying deforestation from remote sensing imagery.

Figure 2: Wind-fallen trees in Stepanavan
(Hayantar, 2014 http://www.hayantar.am)

1.4 Aims and Objectives

This study aims at detection of the forest cover change during a long period of time (1984-present) based on Landsat data. The aim of the study is also to assess the effectiveness of different methods. Achieving these aims entails the following objectives:

- To study if available Landsat data are sufficient for analyzing the patterns and trends of forest in study area
- To obtain temporal trend
- To define forest change spatially

The hypotheses that we yield from the above mentioned objectives are as follows:

1. With the use of Landsat data forest cover change analysis and trend detection can be performed.
2. There is a distinct negative trend in forest cover change.

In order to achieve the above mentioned research goals and objectives, the following research questions need to be reflected on:

- Is it possible to detect patterns and trends of forest changes in local scale using temporally dense Landsat collections? How scientifically robust is the use of those data to identify the changes in the study area taking into account the limitations of study?
- What kind of techniques could be used to analyze forest cover change? Are those methods relevant for research in local scale?
- What is the trend of forest cover change in study area?

1.5 Thesis Organization

Table 1: The summary of the thesis

Is it possible to detect patterns and trends of forest changes in local scale using temporally dense Landsat collections?		PROBLEM
Hypothesis 1 With the use of Landsat data forest cover change analysis and trend detection can be performed	**Hypothesis 2** There is a distinct negative trend in forest cover change	HYPOTHESES
Theoretical study: - Literature - Reading and information gathering - Definition of concepts	**Empirical study:** - Case Study - Performing analysis in Google Earth Engine - Validation	VERIFICATION
Developing the theoretical background which will be the basis for the study		THEORETICAL GOAL
Implementing the algorithm in order to find the forest disturbances during the study period		PRACTICAL GOAL

Table 1 sum up the key points of the thesis. To achieve previously discussed goals and objectives the master thesis consists of six chapters:

Chapter 1: Introduction

Chapter 1 includes the background and the research problem. It comprises the objectives of the study, research questions and gives an idea about the study area.

Chapter 2: Concepts and definitions

Chapter two refers the description of general concepts and definitions that are essential for this research. Furthermore extensive literature review is included, which gives detailed information about the related studies.

Chapter 3: Methodology

Chapter three contains the main methodological approaches and steps that are followed for achieving previously discussed goals. It gives detailed description of study area as well as the data that are used for study. The description of tools and programming environment is also included. The study limitations and constraints are also described in this chapter.

Chapter 4: Data preparation

Chapter four comprises the descriptions of steps of remotely sensed data preprocessing and preparation.

Chapter 5: Detection of forest disturbance and trend analysis

In chapter five the steps of forest change detection and temporal trend analyses are described. There is a detailed description of the vegetation indices that have been used. Afterwards the main steps of implementation of linear regression model and the assessment of the analysis are described.

Chapter 6: Results and discussion

Chapter six summarizes research findings. Main advantages and disadvantages of used methods are discussed. In addition, some recommendations for further analysis are included.

CHAPTER TWO
CONCEPTS AND DEFINITIONS

2.1 The Use of remotely Sensed Data for Forest Monitoring

Various studies have been undertaken in the area of land use and land cover change analysis and particularly for forest change analysis with the use of remotely sensed data. Relating the spectral changes among multi temporal satellite data sets to changes in surface features and biophysical variables has long been an important application of remote sensing technology (Hayes & Cohen, 2007). The increasing availability of remotely sensed data and the improvement of data resolution make it even more useful for forest monitoring.

In general, ecosystems can be described by their condition (their state) and by how they are changing (their temporal dynamics). Remotely sensed data can be successfully used for both purposes across the number of ecosystem types, including forest (Cohen et al., 2004). Forest change mapping and monitoring is feasible when changes in the forest attributes of interest result in detectable changes in image radiance, emitance, or microwave backscatter values (Rogan et al., 2006). Furthermore, the consistent and objective nature of remote sensing measurements allows unbiased comparison of forest disturbances (Griffiths et al., 2012).

Several methods were developed for this aim: manual interpretation, algebraic methods (image differencing, image regression, image ratioing, vegetation index differencing), transformations, thematic classification, post classification change detection, with the use of remotely sensed data from variety of sensors as different states of the land surface can be measured by satellite-derived biophysical parameters (Rogan et al., 2006; FAO 2007; Forkel et al., 2013).

Change detection approaches can be categorized into two broad groups: bi-temporal change detection and temporal trajectory analysis. Almost all classifications for change detection algorithms are based on bi-temporal change detection and little care for temporal trajectory analysis. For bi-temporal images, any kind of change detection algorithm can be attributed to one of the following methods: directly compare different data sources, compare extracted information and detect changes by bringing all the data sources into a uniform model. Temporal trajectory analysis can be decomposed into bi-temporal change detection and long time-series analysis (Jianya et al., 2008).

The most common approaches used in change detection have included the post classification comparison of two dates of land cover classifications and the simple two-date, univariate

differencing of single bands or band ratios. Multivariate techniques that incorporate more spectral information in the change detection algorithm often produce improved results. Examples include clustering of multi temporal composite images and the use of multivariate transformations such as the tasseled cap, principal components analysis and the less used canonical correlation analysis (Hayes & Cohen, 2007).

In their study Hirschmugl et al., (2014) describe the methods that can be used for mapping forest degradation from optical data: simple spectral band values, vegetation indices, proximity to new roads (context analysis), or more advanced tools, such as spectral mixture analysis and related indices, such as the Normalized Difference Fraction Index, or different combinations of these features.

An important issue for forest change detection and analysis is the selection of satellite imagery. The choice of the imagery depends on many factors such as the objectives of the research, characteristics of study area, spatio-temporal resolution of imagery and the costs. If the study is focused on temporal trajectory analysis, forest change analysis is mostly based on low spatial resolution images such as AVHRR and MODIS, which have a high temporal resolution (Jianya et al., 2008).

Another widely used data for forest change analysis is Landsat imagery. The spatial resolution of imagery is informative of human activities on the Earth surface and it has made Landsat invaluable information source for science, management and policy development (Wulder et al., 2011). Forest change detection with Landsat has a history as long as the Landsat program itself (Cohen et al., 2010). The 30 m pixel size of the Landsat TM and ETM+ sensors makes them suitable to characterize the land-cover change resulting from natural and anthropogenic activities.

The number and placement of spectral bands is also an important advantage over other similar sensors and the spectral information of vegetation in Landsat TM and ETM+ imagery is primarily determined by the designation of spectral bands as seen in Table 2. The Thematic mapper (TM) and Enhanced thematic mapper (ETM+) sensors acquire the images in visible, near infrared and shortwave infrared portions of the electromagnetic spectrum, making them appropriate for studies of vegetation properties across a wide range of vegetation communities, in diverse environments (Bhandari et al., 2012). In Table 2 the spectral characteristics of Landsat TM and ETM+ are described (Landsat missions, USGS, 2014). In the first three bands, reflected energy from vegetation is determined by the concentration of leaf pigment. Leaves strongly absorb solar radiation in the visible spectrum, particularly the red spectrum, for photosynthesis. The forth band in near-infrared (NIR) region of solar

spectrum, to which healthy green leaves are highly reflective. In fact, the contrast in leaf reflectance between the red and NIR spectra is a physical basis for numerous vegetation indices using optical remote sensing. The two mid-infrared bands relate to the moisture content in healthy vegetation (Weng, 2011). These two bands are also very sensitive to vegetation density, especially in the early stages of clear cut regeneration.

Table 2: The spectral characteristics of Landsat 4-5 Thematic Mapper (TM) and Landsat 7 Enhanced Thematic Mapper Plus (ETM+)

Band	Wavelength	Useful for mapping
Band 1 - blue	0.45-0.52	Bathymetric mapping, distinguishing soil from vegetation and deciduous from coniferous vegetation
Band 2 - green	0.52-0.60	Emphasizes peak vegetation, which is useful for assessing plant vigor
Band 3 - red	0.63-0.69	Discriminates vegetation slopes
Band 4 - Near Infrared	0.77-0.90	Emphasizes biomass content and shorelines
Band 5 - Short-wave Infrared	1.55-1.75	Discriminates moisture content of soil and vegetation; penetrates thin clouds
Band 6 - Thermal Infrared	10.40-12.50	Thermal mapping and estimated soil moisture
Band 7 - Short-wave Infrared	2.09-2.35	Hydrothermally altered rocks associated with mineral deposits
Band 8 - Panchromatic (Landsat 7 only)	.52-.90	15 meter resolution, sharper image definition

Recent studies (Vogelmann et al., 2012; Verbesselt et al., 2012) introduces to four general categories of vegetative changes, which can be monitored using remotely sensed data:

- abrupt change
- seasonal change
- gradual ecosystem change
- short-term inconsequential change

All four types of changes can alter vegetative spectral properties, and depending on the goals of the investigation, can necessitate the use of different approaches and ancillary data to map them effectively.

Abrupt changes are the result of changes caused by landscape transforming disturbance events, such as those related to logging, deforestation, agricultural expansion, urbanization, and fire. In general, these types of events radically alter the spectral properties of the land surface, and are readily discernible in Landsat imagery.

Seasonal change relates to the cyclical intra- and inter-annual patterns of phenology, whereby seasonality influences vegetation condition in predictable and mostly repeatable patterns of green-up and senescence. Similar to abrupt change, phenological change can have marked impacts on spectral characteristics of the vegetation, and tend to be especially pronounced in deciduous forest.

Gradual ecosystem change relates to subtle within-state changes taking place in vegetation communities that are not related to normal phenological cycles. These include a variety of within state disturbances, such as vegetation damage caused by insects and disease, drought and storms, changes in plant communities related to natural succession, grazing pressure, and climate-induced biome shifts.

The last group of changes is short-term inconsequential vegetative change which is a number of events that cause vegetative spectral changes not perceived as having long-term ecological importance. These include rain-fall events that affect spectral properties of the soil background wind that affects leaf angles during the time of data acquisition), and light frost or snow on conifer vegetation at high elevations, occurring especially during the beginning and end of the growing season. These events may be considered as noise by most analysts as they can have marked impacts on the spectral properties of the data sets being analyzed, which can in turn alter interpretations and create a level of uncertainty in remotely sensed data sets and derived change products. These types of changes tend to be difficult to characterize, and are largely ignored in most change investigations.

Another change that is taking place in forest areas is forest growth which is always a gradual process. Establishment of forest stand always takes time, and trees continue to grow after the stand is established (Weng, 2011).

Vogelmann et al., (2012) discuss the use of Landsat imagery for forest change analysis and they depict that Landsat imagery is applicable for detecting abrupt and gradual ecosystem changes. Landsat is not the ideal sensor for investigations of seasonal changes due to the

difficulty in acquiring enough quality cloud-free data sets to adequately characterize the phenological variability within an ecosystem. Nevertheless, Landsat data provide useful complementary data when used in conjunction with the high temporal resolution data in phenological assessments.

With few exceptions, most research with the use of Landsat imagery have focused on 3–10 years or greater image intervals and one or two Landsat scenes (Cohen et al., 2010). Similar research was also done for north eastern Armenia. Asiryan (2005) shows data analysis for the purposes of forest cover change detection for the surrounding areas of Vanadzor city (north-east Armenia). Two satellite images (Landsat TM/1989 and Landsat ETM+/2000) were processed and analyzed. The results indicated that a significant change in land cover occurred between the 1989 and the 2000. In particular, the analysis revealed the reduction of vegetative cover in the study area.

But as it was shown by Verbesselt et al., (2010), conventional bi-temporal change analysis is not sufficient as most of the methods focus on short image time series. The risk of confounding variability with change is high with infrequent images, since disturbances can occur in between image acquisitions. Similar study clearly highlights the considerable advantages that the annual temporal resolution of the Landsat time series holds over bi- or multi temporal change detection approaches. For example, a change map at five or 10-year interval would not have been able to distinguish a large disturbance occurring in a single year from individual patches clustering to a large area over time (Griffiths et al., 2012).

In addition, although many disturbances often result in abrupt spectral changes that are relatively easy to detect using satellite images acquired before and immediately after each disturbance, the spectral change signals often become obscured and eventually undetectable as trees grow back following those disturbances. As a result, forest change products derived using temporally sparse observations typically have considerable omission error (Weng, 2011). In another study of Verbesselt et al., (2012) was described that detecting changes within time series is the step towards understanding the acting processes and drivers (e.g., natural or anthropogenic). The detailed use of this method is described in the following sections.

2.2 Forest and Deforestation

Before studying the techniques for analyzing spatial and temporal variations of forest, it is important to distinguish the main concepts regarding forest degradation and deforestation. There are many definitions and here some of them are described which gives better insight and understanding of those processes.

1. **Forest**: Moreno-Sanchez et al., (2007) define the terms forest cover or forest to denote high forests (natural or created by plantations) dominated by tree species. The definition of forest is critical for this study as it defines the area where the changes are estimated.

2. **Forest change**: In the context of environmental remote sensing, forest change, manifested as forest attribute modification or conversion, can occur at every temporal and spatial scale, and changes at local scales can have cumulative impacts at broader scales (Rogan et al., 2006).

FAO (2007) specifies the differences of deforestation and forest degradation, which are another crucial terms.

3. **Deforestation**: The conversion of forested areas to non-forest land use such as arable land, urban use, logged area or wasteland. According to Food and Agriculture Organization of the United Nations (FAO), deforestation is the conversion of forest to another land use or the long-term reduction of tree canopy cover below the 10% threshold. Deforestation defined broadly can include not only conversion to non-forest, but also degradation that reduces forest quality - the density and structure of the trees, the ecological services supplied, the biomass of plants and animals, the species diversity and the genetic diversity. Narrow definition of deforestation is: the removal of forest cover to an extent that allows for alternative land use.

4. **Forest degradation**: The process leading to a temporary or permanent deterioration in the density or structure of vegetation cover or its species composition. It is a change in forest attributes that leads to a lower productive capacity caused by an increase in disturbances. The time-scale of processes of forest degradation is in the order of a few years to a few decades. In another study forest degradation was described as a reduction in the natural or desirable characteristics of a forest (e.g. age, classes, structure, density, or standing stock genetic quality) (Moreno-Sanchez et al., 2005). Taking into account the specialties of the study area and particular forest variations, this study is focused on detection of disturbances causing forest degradation.

5. **Reforestation:** Re-establishment of forest formations after a temporary condition with less than 10% canopy cover due to human-induced or natural perturbations. The definition of forest clearly states that forests under regeneration are considered as forests even if the canopy cover is temporarily below 10%. Many forest management regimes include clear-cutting followed by regeneration, and several natural processes, notably forest fires and windfalls, may lead to a temporary situation with less than 10 percent canopy cover. In these cases, the area is considered as forest, provided that the re-establishment (i.e. reforestation) to above 10 percent canopy cover takes place within the relatively near future. As for deforestation, the time frame is central. The concept temporary is central in this definition and is defined as less than ten years.

2.3 Time Series Analysis

The recent opening of the global Landsat archive by the United States Geological Survey (USGS) provides new opportunities to advance land use science and has sparked the development of new methodological approaches. For example, change detection methods based on annual Landsat time series (i.e. trajectory-based change detection methods) make better use of the temporal depth of the Landsat archive to reconstruct forest disturbance histories with annual resolution and to map trends, such as forest regeneration and succession. Likewise, annual time series of Landsat images can help to separate sudden from gradual vegetation change (Griffiths et al., 2012). Cohen et al., (2010), mentions about tremendous need for temporally and spatially detailed forest change information over vast areas for forest management and policy considerations.

Estimating change from remotely sensed data series however is not straightforward, since time series contain a combination of seasonal, gradual and abrupt ecosystem changes occurring in parallel, in addition to noise that originates from the sensing environment (e.g., view angle), remnant geometric errors, atmospheric scatter and cloud (Verbesselt et al., 2012).

One of the algorithms is a trajectory based change detection algorithm developed by Kennedy et al., (2007). The main premise of the method is the recognition that many phenomena associated with changes in land cover have distinctive temporal progressions both before and after the change event, and that these lead to characteristic temporal signatures in spectral space. Rather than search for single change events between two dates of imagery, they instead searched for idealized signatures in the entire temporal trajectory of spectral values. If an area fitted the idealized trajectory according to a simple least-squares measure of goodness of fit, it

is likely to have experienced the phenomenon described by that trajectory. Because the entire trajectory was considered, the method utilized the depth of rich image archives, and because detection was based on the fit of a curve, thresholds were based on a statistical metric that is internally calibrated to each pixel, avoiding the need for manual interpretation or intervention. Another study shows validation of North American forest disturbance dynamics derived from Landsat time series stacks with biennial time steps. For further analysis they use vegetation change tracker (VCT) algorithm specifically for mapping forest change using Landsat time series stuck or data sets that consist of temporally dense satellite acquisition. The algorithm consists of two major steps: 1) individual image analysis and 2) time series analysis (Thomas et al., 2011).

Griffiths et al., (2012) discuss, that the analysis of an annual Landsat time series with trajectory-based change detection methods (such as LandTrendr) can provide deep insight into the effects of the institutional and socioeconomic changes on forests.

Another complex approach is proposed for automated change detection in time series by detecting and characterizing Breaks For Additive Seasonal and Trend (BFAST) by Verbesselt et al., (2010). BFAST integrates the decomposition of time series into trend, seasonal, and remainder components with methods for detecting significant change within time series. BFAST iteratively estimates the time and number of changes, and characterizes change by its magnitude and direction. They tested BFAST by simulating 16-day composites of Normalized Difference Vegetation Index (NDVI) time series with varying amounts of seasonality and noise, and by adding abrupt changes at different times and magnitudes. This revealed that BFAST can robustly detect change with different magnitudes (>0.1 NDVI) within time series with different noise levels (0.01–0.07 σ) and seasonal amplitudes (0.1–0.5 NDVI) (Verbesselt et al., 2010).

In several studies (Jin & Sader, 2005; Cohen et al., 2010; Verbesselt et al., 2012, Vogelmann et al., 2012; Forkel et al., 2013), trends in forest area were analyzed through image-derived vegetation index and transformations.

Forest disturbances and their subsequent regeneration are often detected and mapped using spectral indices. These indices are mostly based on the short wave infrared (SWIR) and near infrared (NIR) reflectance, although forest disturbances can also be detected in the visible or thermal spectrums. NIR reflectance decreases with an elevated defoliation level and/or after forest dieback, because bark and soil reflectance is lower than the reflectance of needles or leaves. Disturbance detection may be complicated when the understory vegetation is not removed (e.g., by tree defoliation). The understory has a high NIR reflectance and thus may

compensate for the decrease in NIR reflectance resulting from forest disturbance. In contrast, the SWIR reflectance of forest stands is lower than that of the bark, soil, and understory, so SWIR reflectance increases after forest disturbance (Hais et al., 2009).

Literature is replete with the most frequently used approach for detecting temporal trends: fitting linear regressions of a (temporally aggregated) vegetation index (VI) against time (Jong & Bruin, 2012). Vogelmann et al., (2012) describe the use of linear regression relationships on a pixel by pixel basis between time (x variable) and the vegetation index value (y variable) for selected pixels. They delineate that regression models with low slope value tend to not be statistically significant (no apparent change), whereas the models with high positive or negative slope values are more likely to be statistically significant. Results from this study indicate that analyses of Landsat time series data provide useful perspectives regarding long-term gradual ecosystem changes taking place across landscapes. All investigated areas showed evidence of significant trends in spectral change associated with the gradual loss and accrual of vegetation canopy cover.

Change detection, however, is often complicated by a number of statistical preconditions that are intrinsic to time series of spectral vegetation indices with dense sampling intervals, but this needs to be done with care in order to avoid spurious trends. The detected slope can be used to calculate the amount of change, but it is not always tested for significant deviation from zero, nor standard statistical assumptions always respected. Seasonal variation is an important cause for the data to violate assumptions like homogeneous variation and absence of serial correlation in the residuals. In few cases linear models were fitted directly to seasonal data, but seasonality is typically remediated using temporal aggregation, where the aggregation window corresponds to the length of a calendar year.

Large variation in detected changes was found for aggregation over bins that mismatched full lengths of vegetative cycles, which demonstrates that aperiodicity in the data may influence model results. Using VI data and aggregation over full-length periods, deviations in VI gains of less than 1% were found for annual periods (with respect to seasonally adjusted data), while deviations increased up to 24% for aggregation windows of 5 year. This demonstrates that temporal aggregation needs to be carried out with care in order to avoid spurious model results.

The risk of artefacts is minimal at an aggregation level corresponding to a full period, for instance a calendar year. Coarser aggregation levels tend to overestimate the amount of change and result in higher variation in model predictions, especially from 3 periods onwards. However, the use of a full-period window may be impractical because VI time series are

hardly ever free of changes in seasonality. Aperiodicity within long-term time series of vegetation indices is intrinsic to certain land cover types and may arise from variations in start and length of growing seasons as a result of variations in temperature and/or precipitation (Jong & Bruin, 2012).

In a latest study of Hansen et al., (2013) it was shown the use of time-series analysis of 654,178 Landsat 7 ETM+ images in characterizing global forest extent and change from 2000 through 2012. As a result tree cover, forest loss, and forest gain was shown during the study period. Percent tree cover, forest loss and forest gain training data were related to the time series metrics using a decision tree. Forest loss was disaggregated to annual time scales using a set of heuristics derived from the maximum annual decline in percent tree cover and the maximum annual decline in minimum growing season NDVI. Trends in annual forest loss were derived using an ordinary least squares slope of the regression of annual loss versus year. This study has significant role in forest change analysis because it has global coverage and the results can serve for validation of the current study.

Given the limited availability of cloud free Landsat data in some areas of the globe, epochal composites have been used extensively to support change detection studies. These composites represent a new paradigm in remote sensing that is no longer reliant on scene-based analysis (White et al., 2014).

A time series of these image composites affords novel opportunities to generate information products characterizing land cover, land cover change, and forest structural attributes in a manner that is dynamic, transparent, systematic, repeatable, and spatially exhaustive.

White et al., (2014) proposes three unique types of pixel-based image composites:

- annual (single-year) composites,
- multi-year composites,
- proxy-value composites.

Annual composites are surface reflectance composites that use the best available pixel observation (from the target year) for any given pixel location. Annual composites are produced using a set of specified rules that are defined according to the information need. For example, an annual composite may be designed to capture a specific time period or a limited phenological window. In addition to a day-of-year rule, rules may also constrain observations according to sensor, distance to cloud and cloud shadows, and atmospheric opacity (to reduce the impact of haze). If there are no observations that satisfy the compositing rules for a given pixel location, then the pixel is coded as "no data" and as a result, annual composites may have areas of missing data.

Multi-year composites are generated according to a set of user-specified rules; however, pixel observations from previous or subsequent years may be used when no suitable observation is found within a desired target year.

Proxy value composites are annual composites where no data pixels are populated using a time series of annual composites to determine proxy values. Likewise, pixels with anomalous values those that exceed a pre-defined range of expectation or which have opacity values indicative of hazy imagery may also be assigned a proxy value. In essence, the objective of the proxy value composite is to assign the most similar value in time and space to a pixel that either has no data or has an anomalous value.

CHAPTER THREE
METHODOLOGY

3.1 Workflow

From the review of other researches in the preceding chapter, it is logical to deduce that temporally dense satellite data can give better idea about trend in forest dynamics.

Based on related studies the main steps of research were developed:

- Data preparation and image preprocessing
- Image processing
- Detection and analysis of long term trend
- Evaluation of spatial distribution of forest change
- Validation of results

The goal of preprocessing is to ensure that each pixel faithfully records the same type of measurement at the same geographic location over the time. Preprocessing is especially critical in change studies because the detection of change assumes that the spectral properties of non-changed areas are stable, and inadequate pre-processing can increase error by causing false change in spectral space (D. Lu & Q. Weng, 2007). This step includes radiometric corrections and cloud and shadow masking.

Several studies have shown the impact of clouds and cloud shadows on vegetation change analysis. The pixels contaminated with cloud and shadow generally have sufficiently different reflectance properties than the actual land cover and produce erroneous information if used in an automated mapping algorithm (Bhandari et al., 2012). To eliminate this effect cloud masking function is implemented over the image collection.

The data preparation step also includes the creation of image composites. Characteristics relevant to particular geographic regions, such as persistence of cloud cover, topography, dynamism of landscape processes, phenology, and Landsat data availability, are important considerations when applying a compositing approach. Likewise, different information needs (e.g., disturbance mapping, estimation of biophysical parameters) may dictate different compositing strategies, target dates, and compositing rules that are specific to the application. In general, it is desirable to generate composites that have consistent phenology with minimal no data pixels that best represent the phenomenon of interest (e.g., land cover classes, forest structural attributes, or specific disturbance events).

Pixel-based image compositing of Landsat data has emerged from a unique confluence of scientific and operational developments, predicated by free and open access to the Landsat archive, and supported by computing and data storage capacity to fully automate radiometric and geometric pre- processing and create increasingly robust standardized image products (White et al., 2014).

Many studies, like Cohen et al., (2010) stated, that the use of dense (nearly annual) Landsat time series allows characterization of vegetation change over large areas at an annual time step and at the spatial grain of anthropogenic disturbance. Additionally, it is more accurate in detection of subtle disturbances and improved characterization in terms of both timing and intensity. Based on this, time series of Landsat images will be created. It is worth to mention, that timing and the variation of vegetation phenology should be considered and as a result, the images should be chosen from the same time of the year and particularly from peak growing season (early June to late September). It is stated that images acquired outside this temporal window are generally not suitable for forest change analysis, because leaf off deciduous forests can be spectrally confused with disturbed forest land. (Weng, 2011).

Time series of vegetation indices (VI) derived from satellite imagery provide a consistent monitoring system for terrestrial plant productivity. They enable detection and quantification of gradual changes within the time frame covered. The dependent variable Y can be any kind of VI or cyclical environmental parameter in general. (Jong & Bruin, 2012).

For this study we used the NDVI, which is a commonly used proxy for terrestrial photosynthetic activity. To detect the partial harvests with better accuracy NDMI is also used. The following step is temporal trend analysis. Time series analysis of the rate of change of forest area is calculated using the slope estimate from linear regression. The slope indicates the strength of a trend in the change of forest. (Google Earth Engine API tutorial, 2014).

The spatial patterns and the distribution of forest change can be studied by using the results from image processing step. Afterwards the results are validated by comparing with ground truth forest harvest data and the data from yearly reports of annual reports of State forest monitoring center of Armenia (http://www.forest-monitoring.am/).

3.2 Study Area

The study area is located in the north-eastern part of Armenia. The Republic of Armenia is located in southwest Asia. The country has a total area of 29 800 km^2 (Moreno-Sanchez et al., 2005). Armenia is situated in a dry subtropical climatic zone. Annual precipitation ranges from 250-300 mm to 1 000 mm. In this dry-subtropical region, forests play a major role in preserving favorable environmental conditions for sustainable development (Sayadyan & Moreno-Sanchez, 2006).

The terrain complexity and microclimatic diversity, as well as the fact that Armenia is located at the crossroads of four different floristic provinces (Old-Mediterranean, Near-east Asian, Iran-Turanian and Caucasian), produce different vegetation types with high biodiversity and high percentages of plant and animal endemism. Today the country is included in the Caucasus and Irano-Anatolian biodiversity hotspots. The dendroflora is composed of 110 tree and 152 bush species. The Armenian forests are predominantly composed of complex mixes of broadleaf deciduous tree species (mostly Oak *Quercus spp.*, beech *Fagus orientalis*, and hornbeam *Carpinus betulus* and *C. orientalis*) (Moreno-Sanchez et al., 2007).

Today the Armenian forests can be characterized as overstocked and over-mature forests with low density, low annual growth rates, and poor regeneration. Figure 3 represent the forest types in Armenia.

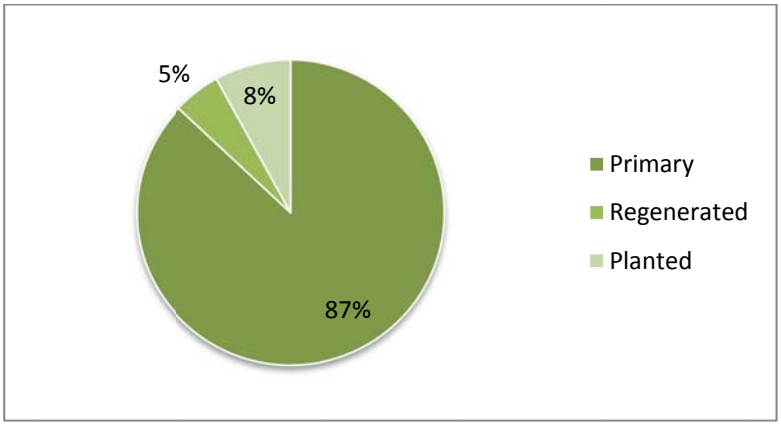

Figure 3: Types of forest in Armenia (Global Forest Watch, Armenia, http://www.globalforestwatch.org/country/ARM)

The north-eastern and south-eastern parts of the country and the eastern bank of Lake Sevan have the most favorable climatic and environmental conditions for the growth of forests. Most Armenian forests are found in mountainous terrain between 500 and 2200 m above sea

level. The forest cover is highly fragmented. The 62% of the forest cover is found in the northeast (Moreno-Sanchez et al. 2005). This was the primary reason of the study area choice, due to the fact that forests are mostly located in this part of the country, and as stated by Asiryan, (2005) this areas have suffered damage made over the last twenty years.

The transformations and current state of the Armenian forests result from decades of management policies and forest use practices by several stakeholders and economic activities. Planned industrial production or use of the forests was very limited during the Soviet and independence periods (Moreno-Sanchez et al., 2007). The pressure on forest as a source of fuel abruptly increased after the independence due to economic blockage. Starting from these years the forest logging was uncontrolled. There was an attempt by authorities to control the forest harvest in order to lower the damage caused by cuts. To do so plans were made to supply fuel wood to the population during 1993. Before 1993, the fuel wood cut was fixed at 60 000 m^3 per year. As a result, in 1993 the harvest was raised to 100 000 m^3. In reality, this plan was difficult to realize because of fuel limitations, and the transportation of the wood to distribution areas was a major impediment. Estimates of the volume of the illegal cutting suggest that 700 000-1 000 000 m^3 of wood were cut illegally in each of three winters 1992-1995 (Sayadyan, 2007).

Thurresson et al., 1999 stated that forested areas close to population centers became the main source of fuel wood during the winters of 1991-1993 and were heavily damaged. Legal and illegal cuttings during 1991-1996 are estimated around 600 000 m^3 per year.

Illegal logging in Armenia is conducted mainly by local communities for survival through unauthorized timber extraction from the state forests. The timber consumed by rural households was estimated to be 568 000 solid m^3 annually. The overall timber production was estimated 847 000 solid m^3 in 2003, from which officially allowed and registered volume constituted 63 000 m^3. Thus cuttings in average is 1 000 000 m^3/year, which makes 13 000 000-14 000 000 m^3 for last 13-14 years (Sayadyan, 2007).

According to “Hayantar” organization of the Ministry of Agriculture of the Republic of Armenia, which is the main organization responsible for conservation, protection, reproduction, use, registration and sustainable use of forest resources, currently there are 19 forest units. For research, 9 forest units and 1 national park were chosen. The 9 forest units are Ijevan (20955.8 ha), Dsegh (14505.2 ha), Gugarq (10496.9 ha), Sevqar (18236.5 ha), Arcvaberd (38664.2ha), Noyemberyan (27001 ha), Lalvar (24339.5ha), Jiliza (13851.1ha), Tashir (5105.2 ha) and Dilijan national park (24000 ha) with more than 190 000 ha (1900 square km) total area of forest. The area comprises the biggest and compacted part of

Armenia's forest cover. Also this area is described as one of the most vulnerable to degradation. Figure 5 illustrates the location of study area in Armenia.

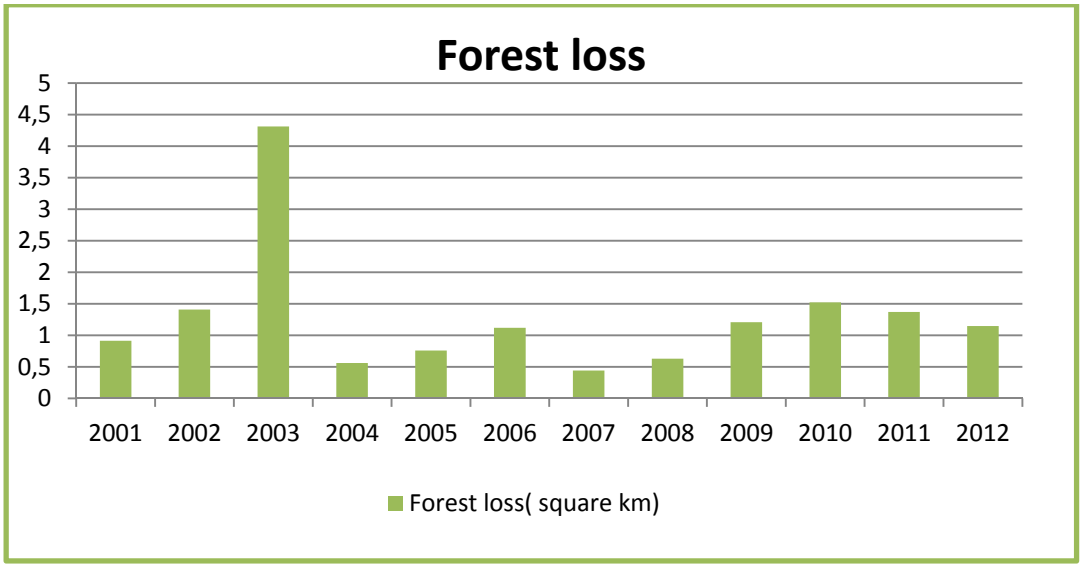

Figure 4: Forest loss in the study area (Hansen et al., 2013)

Figure 4 approximates the forest loss evaluated by Hansen et al., (2013). The data were accessed directly in GEE and tree loss per year was computed for the area of interest. All the other numbers and estimates are covering the forest loss in the overall area of Armenia. Those estimates are relevant, as the most of the forests are located in northeast. Figure 4 provides additional insight about forest dynamics specifically in the study area. It is worth mentioning that forest loss evaluated by Hansen et al., (2013) have depicted considerably small value of loss in 2001-2012 (the small values can be accounted for by the global algorithm) but still it can give an idea about the trends and fluctuations of forest loss in northeastern Armenia.

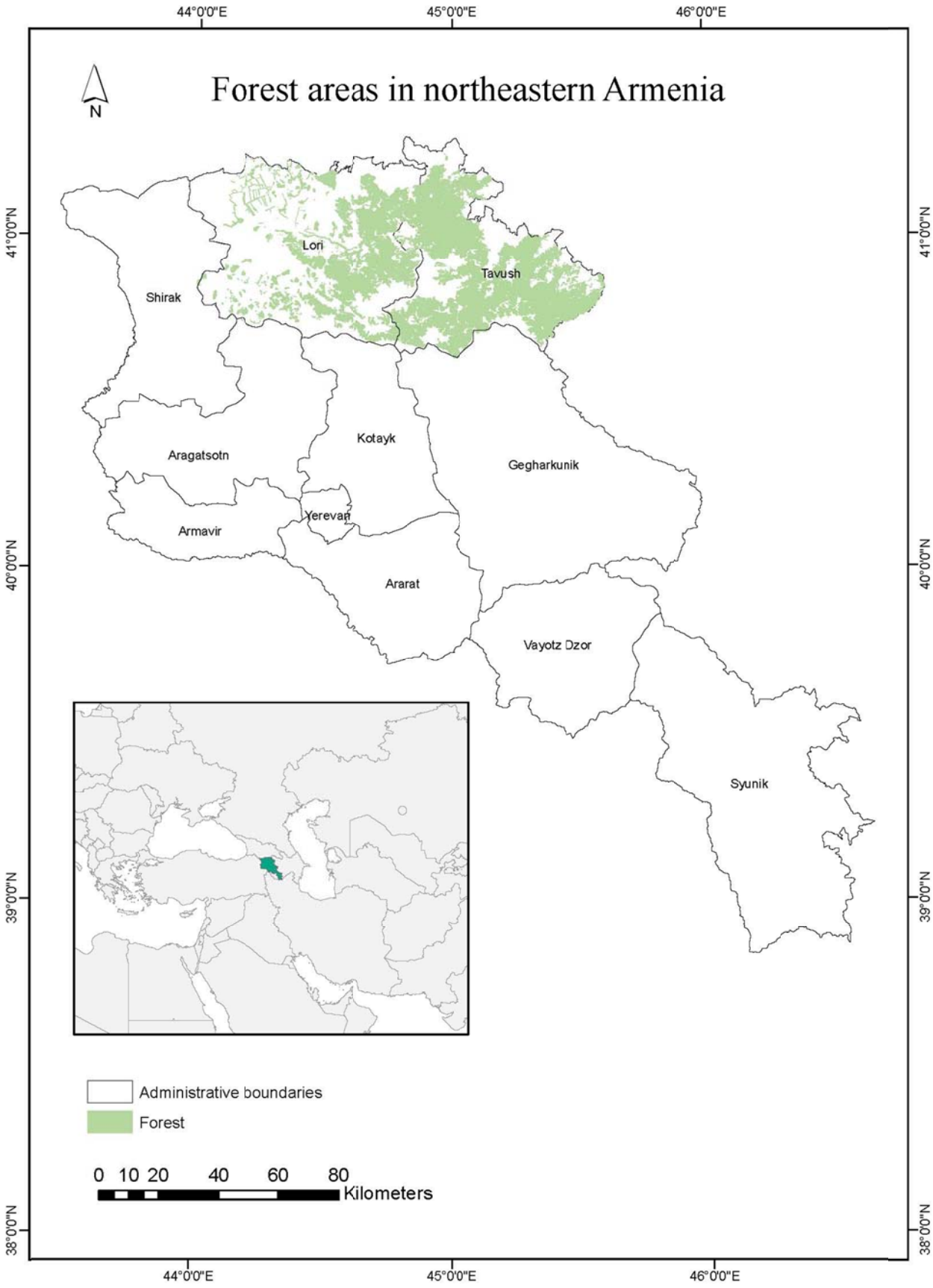

Figure 5: Location map of the study area

3.3 Materials and Tools

For the study Landsat image collections are used. Data are accessed form Google's public catalog, which contains a large amount of publicly available georeferenced imagery, including most of the Landsat archive (Google Earth Engine. API tutorial, 2014).

For study two image collections are chosen from Landsat TM and ETM+ sensors. Table 3 presents the main parameters of image collections. It should be stressed that data availability is presented for whole collection and imagery can be unavailable for specific regions and time period. As far as this study area is concerned, the data are missing for several years.

The choice of Landsat is conditioned by several advantages. First, mission continuity: Landsat offers the longest-running time series of systematically collected remote sensing data. Second, the spatial resolution of the data facilitates characterization of land cover and the change associated with the grain of land management (Cohen & Goward, 2004), and the last, the affordability of data.

Table 3 : Description of used imagery

Data type	Landsat TM	Landsat ETM+
Image collection ID	LANDSAT/LT5_L1T_TOA	LANDSAT/LE7_L1T_TOA
Spectral resolution	7 bands	8 bands
Spatial resolution Panchromatic /multispectral /thermal	/30 meters /60 meters	15 meters/30 meters/60 meters
Radiometric resolution	8 bit	8 bit
Temporal resolution	16 days	16 days
Data availability	Jan 1, 1984 - May 5, 2012	Jan 1, 1999 - Oct 3, 2014

Above mentioned data collections provide data with Level L1T orthorectified scenes, using the computed top-of-atmosphere reflectance. The images are chosen from leaf-on vegetation season (early June-late September). In order to have continuous time series Landsat 7 SLC-off images are also included (years after 2003).

Remote sensing data preprocessing and analysis are carried out in Google Earth Engine JavaScript API. Google Earth Engine (GEE) is an online environmental data monitoring platform that incorporates data from the National Aeronautics and Space Administration (NASA) as well as the Landsat Program. After the USGS opened access to its records of Landsat imagery in 2008, Google saw an opportunity to use its cloud computing resources to allow records of Landsat imagery to be accessed and processed over its online system. This has enable users to reduce processing times in analyses of Landsat imagery and make global scale Landsat projects more feasible (e.g., Hansen et al., 2013). The advantages of GEE can be summarized as:

- Easily accessible satellite imagery and vectors
- Methods for performing analyses with those data
- Parallelized and run in the Google cloud

Earth Engine JavaScript API can be used for programmatically access and analyze vast amounts of geospatial data. We want to stress that the Earth Engine API and advanced Earth Engine functionality at http://earthengine.google.org/ are experimental and subject to frequent change and are restricted to Earth Engine Trusted Testers. For this, Earth Engine Beta tester access was acquired (Google Earth Engine. API tutorial, 2014).

3.4 Research Limitations

Although Landsat images seem potentially useful for this research, we encountered several limitations that made it rather difficult to carry on.

1. Availability of Landsat images

As the main objective is the analysis of temporal and spatial variations of forest, dense Landsat data are required. Unfortunately, there is a time gap from 1988 to 1998.

2. The quality of images

In order to have continuous time series Landsat 7 SLC-off images are also included to collection (years after 2003). On May 31, 2003, the Scan Line Corrector (SLC), which compensates for the forward motion of Landsat 7, failed. This makes data affected by

missing scan lines, particularly the SLC-off effects are most pronounced along the edge of the scene (Landsat missions, USGS, 2014).

Another concern is cloud contamination of images, as Landsat images are highly affected by atmospheric conditions. The study area is regularly cloudy and there are years, when there are only 1 or 2 available cloud free images for the whole year. As a result several images cannot be used for research because of extensive cloud cover, which makes the real number of potentially useful imagery very small. To overcome these obstacles, Landsat compositing methods, cloud masking operations are used.

3. Availability and access to forest monitoring data

Although there are some publications about the forest and the disturbances the critical problem in this research field is the lack of continuous data. Furthermore, the data are poorly published and frequently hard to get from public authorities.

CHAPTER FOUR
DATA PREPARATION

4.1 Image Preprocessing

From the review of related studies, it was concluded, that the results of time series analysis of satellite imagery and the detection of changes highly depend on the accuracy of image preprocessing steps and the homogeneity of satellite imagery. There are numerous steps described in literature for achieving this aim and for creating images applicable for further trend analysis. Figure 6 illustrates the main steps that are performed.

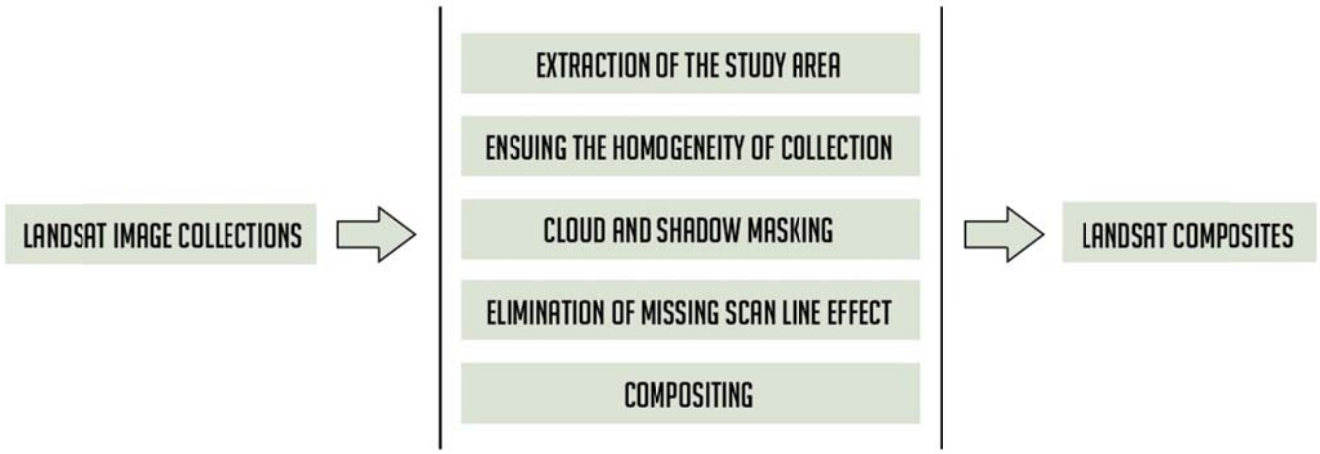

Figure 6: Flow chart of preprocessing steps

Extraction of the study area

The first step towards data preparation is the extraction of the area of interest. It was mentioned before, that most of the analyses in Earth Engine take place on collections of images. Earth Engine has hundreds of image collections including all Landsat archive, which gives a unique opportunity to use Landsat's temporal depth. It is possible to create custom collections by filtering large datasets to include selected scenes. The advantage of Earth Engine is that it automatically mosaics images together, making it easy to perform operations on large datasets. To extract the study area simple reducer is applied, which minimizes the

collection by the polygon of study area. Figure 7 ilusstrates raw Landsat composite which is resulted from clipping.

Ensuing the homogeneity of collection

Landsat images available in GEE had already been orthorectified (L1T level). The L1T level mean, that they provides systematic radiometric accuracy, geometric accuracy by incorporating ground control points, while also employing a Digital Elevation Model (DEM) for topographic accuracy (Landsat missions, USGS, 2014). Co registration of images was manually checked to ensure that images are geometrically corrected. As the images had high accuracy of registration acceptable for this research, further steps for geometric corrections were not performed. To assure the comparability of results across different Landsat sensors and for calibrating images from various sensors the digital numbers should be converted to a commonly used radiometric scale. The selected image collections are calibrated to top-of-atmosphere reflectance. During calibration, pixel values from raw, unprocessed images are converted to units of absolute spectral radiance using 32-bit floating-point calculations. The absolute radiance values are then scaled to 8-bit (TM and ETM+, Qcalmax = 255) numbers representing Qcal (calibrated digital numbers) before creating the output image. We selected only images from the peak growing season (early June – late September) in order to eliminate the effects of seasonal variations of vegetation.

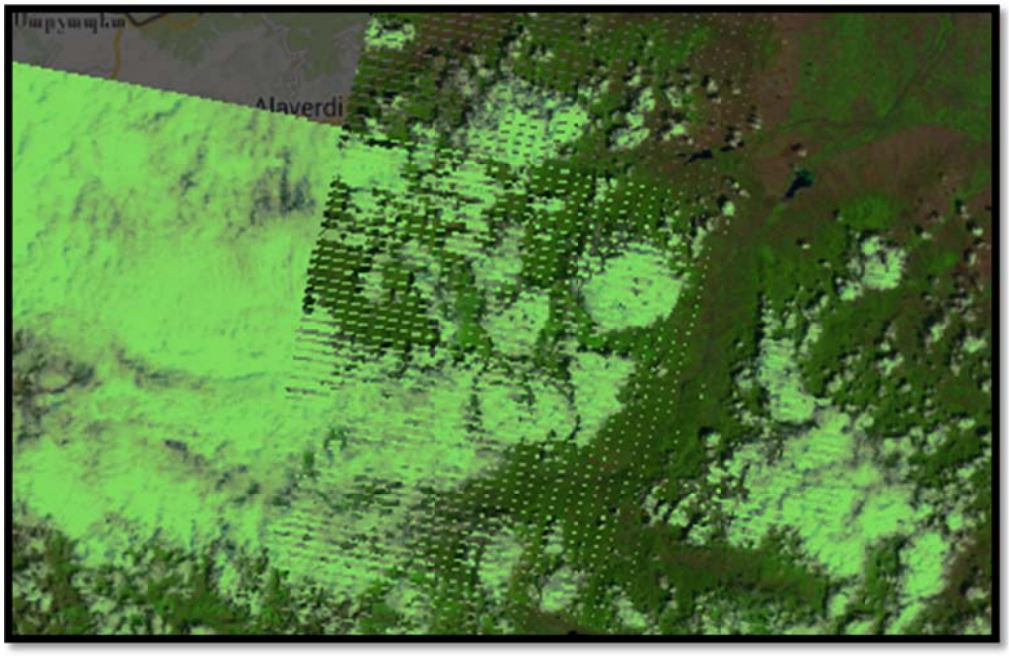

Figure 7: False color composite of Landsat image of year 2003

Cloud and shadow masking

Cloudy pixels generally have different spectral signatures. If unflagged, most likely they will be mapped as non-forest regardless of the actual surface conditions beneath the clouds. For forest change analysis, unflagged clouds over forests likely will be mapped as forest disturbance. Cloud shadows over forests may also be mapped as disturbance, because as the spectral signature of forest under shadow can be significantly different from that of sunlit forest (Weng, 2011).

For masking clouds and shadows Lansat.SimpleCloudScore algorithm is used, which is one of the advanced functionalities available in GEE. It computes a simple cloud-likelihood score in the range [0,100] using a combination of brightness, temperature, and NDSI. Simple cloud score is not a robust cloud detector, and is intended mainly to compare multiple looks at the same point for relative cloud likelihood (Google Earth Engine. API tutorial,2014).

With assigning a threshold of clouds 20, clouds are filtered and masked. Cloud masking operation significantly reduced the data. Figure 8 represents the image of 2003 after cloud and shadow masking. We can notice significant reduction of data.

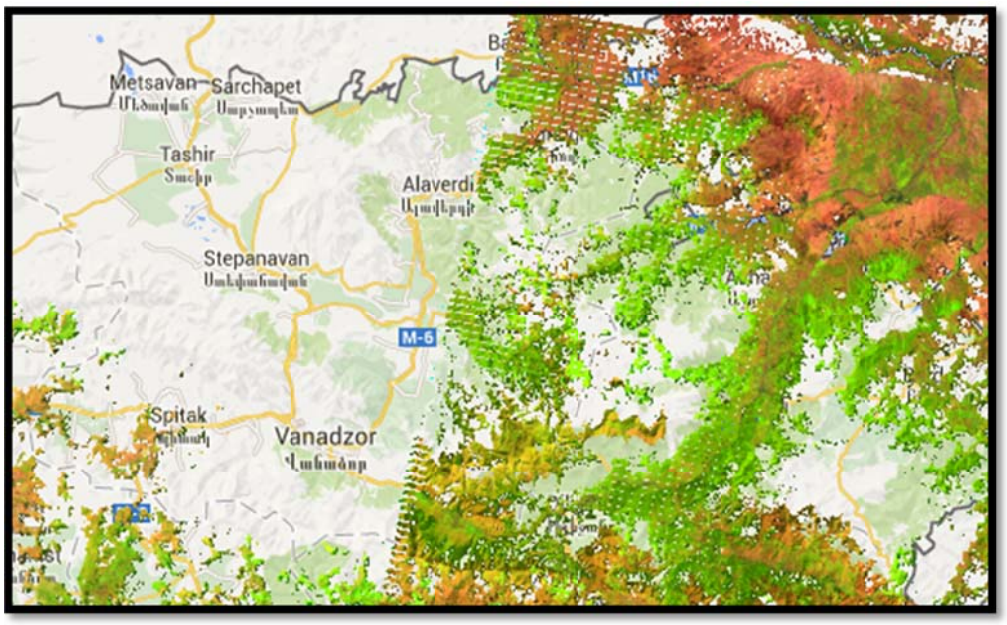

Figure 8: False color composite of Landsat image of year 2003 after cloud and shadow masking

Elimination of missing scan line effect

The following step is the reduction of missing scan line effect. For this purpose simple function was mapped on collection which masked out the anomalous data along the edges of Landsat scene.

Compositing

It was discussed in previous chapters that one of the significant limitations of study is the availability and quality of Landsat imagery. The creation of composites is rather challenging for the study area due to the limited number of available scenes.

A number of rules were applied in order to generate cloud-free, radiometrically and phenologically consistent image composites that are spatially contiguous over large areas. This shift from a scene-based perspective to a pixel-based perspective for image understanding and processing is key, and mirrors trends and developments in time series analysis approaches (White et al., 2014).

In summarizing temporal trends, an important question arises with regards to the length of the time interval used for the summaries. The interpretability of simple shape parameters, such as slope and curvature, will depend on the length of time over which the trend is calculated (Lehmann et al., 2013).

As the most of forest change studies focus on annual change detection, we first tried to create yearly composites. Because of reduced data, these composites were not suitable for further analysis. Figure 9 shows the composite of year 1985 where substantial part of data is missing.

4.2 The Results of Data Preparation

The examples of data inconsistency (Figure 9) and reduction due to preprocessing steps (Figure 8) shows that annual composites didn't cover whole study area. It was concluded, that the data are not sufficient for consistent annual compositing. Instead of that, two-year composites were created.

The results of data preparation step are 10 cloud free surface reflectance composites that use the available pixel observation for given location. The composites are produced using a set of specified rules that are defined according to the information need: they capture a specific time period during a limited phenological window of dry season. Bi-annual time series of

Figure 9: False color composite of Landsat image of year 1985

Landsat TM/ETM+ images are acquired for the periods 1984-1987 and 1999–2014. The resulting composites are free of clouds and homogeneous in appearance. Although the effects of missing scan lines are still noticeable, the composites have considerably better quality and are suitable for further analysis (Figure 10).

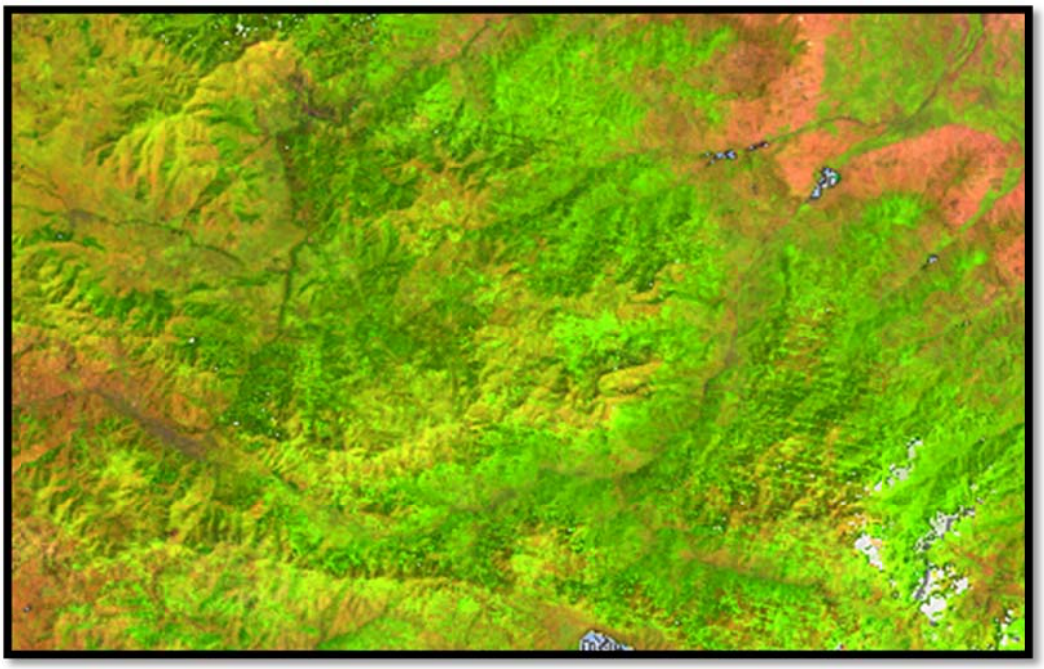

Figure 10: False color composite of Landsat image of years 2003-2004

CHAPTER FIVE

DETECTION OF FOREST DISTURBANCE AND TREND ANALYSIS

5.1 Image Processing

The resulting composites for the periods 1984-1987 and 1999–2014 were used in a linear trend analysis to characterize spatio-temporal patterns of forest cover changes. For that 2 vegetation indices were used and added to composites. To process the trend analysis, time band was also added, which append the time properties of composites.

It is described in previous chapters, that two types of forest disturbances are taking place in study area: clear cuts and selective logging. For this research, two simple, yet efficient vegetation indices are used Normalized Difference Vegetation Index (NDVI) and Normalized Difference Moisture Index (NDMI). Clear cuts can be detected with acceptable accuracy using either NDMI or NDVI. However, partial harvests usually are detected with lower accuracy (especially using NDVI). To assess the partial harvests with higher accuracy, NDMI was used. In the following section both indices will be described.

The NDVI technique for monitoring vegetation greenness and biomass is a well-known and commonly used method in forest change detection (Wilson & Sader, 2002).

NDVI is defined as:

(Band 4−Band 3) / (Band 4+Band 3),

Band 4 is the reflectance of Landsat TM or ETM+ near-infrared band 4, and band 3 is reflectance of Landsat TM or ETM+ red band 3. NDVI separates green vegetation from other surfaces because the chlorophyll of green vegetation absorbs red light for photosynthesis and reflects the near-infrared wavelengths due to scattering caused by internal leaf structure. Thus, high NDVI values indicate high leaf biomass, canopy closure, or leaf area. The ease of calculating NDVI from various types of satellite data, the success of the NDVI in detecting vegetation, and its ease in calculation and interpretation has made it a popular spectral vegetation index, as well as a widely used data product for studying vegetation (Wilson & Sader, 2002).

Index values can range from -1.0 to 1.0. Higher index values are associated with higher levels of healthy vegetation cover, and vice versa, non-vegetation cover (soil, rocks) produces negative values (Asiryan, 2005).

To improve the detection of selective logging the NDMI is used, which is derived from the Landsat TM or ETM+ near infrared band 4 and the short wave infrared band 5 and can be defined as:

(Band 5−Band 4) / (Band 5+Band 4),

Several studies report, that the SWIR bands, compared to others, explained more information about forest structure in conifer and hardwood forests. Although few vegetation studies have applied the NDMI, it is reported that the NDMI was highly correlated with canopy water content and more closely tracked changes in plant biomass than did the NDVI. Compared NDMI and NDVI to detect forest changes at different Landsat acquisition intervals, in all classification trials, the NDMI change maps had a higher overall accuracy than the NDVI change maps. The higher accuracy of the NDMI change maps was due to an increased ability to detect lighter disturbances including partial cuts (Wilson & Sader, 2002; Jin & Sader, 2005).

5.2 Trend analysis

To analyze the trends in forest area, simple linear regression model was used. Ordinary least squares regression was performed, where the linear model was fitted to values of each pixel. The independent variable in the model was the time and the dependent variable was the values of indices for each pixel. Afterwards the slope of the regression was spatially aggregated.

Earth Engine currently supports one trend analysis method, formaTrend. FormaTrend can be used to compute either the long and short term trends of a time series or the trends of the ratio of the time series and a covariate. The long term trend is estimated from the linear term of a regression on the full time series. FormaTrend acts on an image collection, or time series, to extract trends.

Given two time series, the predictors and the responses, formaTrend:

1. Sorts both time series by time,
2. Linearly interpolates predictor values to the time base of the responses,
3. Replaces masked values with the nearest unmasked value,
4. Replaces times with an observation number,
5. Computes the OLS on the resulting vector (Google Earth Engine. API tutorial, 2014).

The following figures (Figure 11 and 12) illustrate the visualization of long term trends of NDVI and NDMI. To visualize the trends color ramp from red to green was used, where with

shades of red are illustrated the decrease of the vegetation (negative slopes) and the linear increase of vegetation is represented with shades of green (positive slopes).

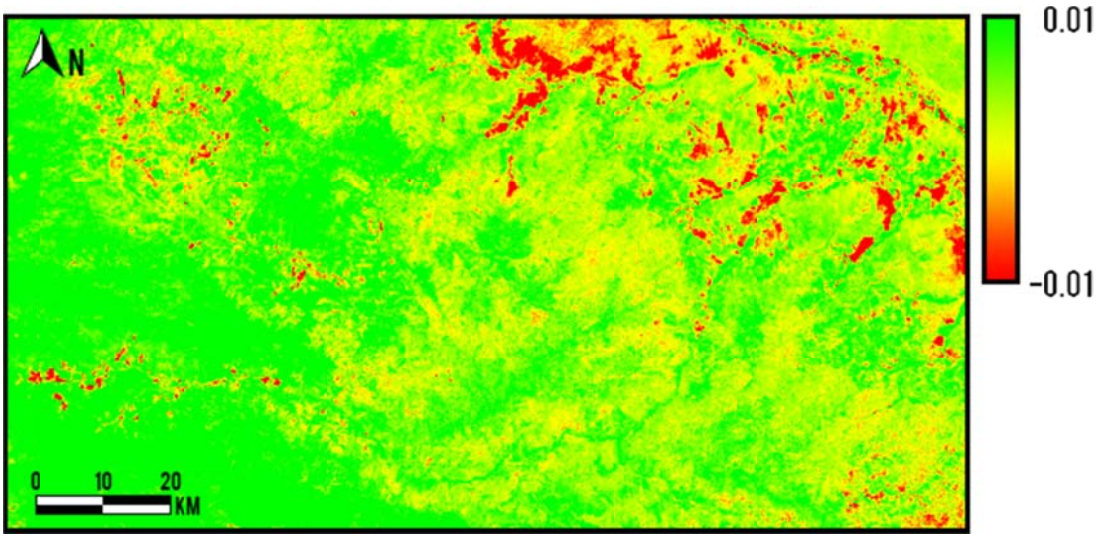

Figure 11: Long term trends of NDVI (using FormaTrend)

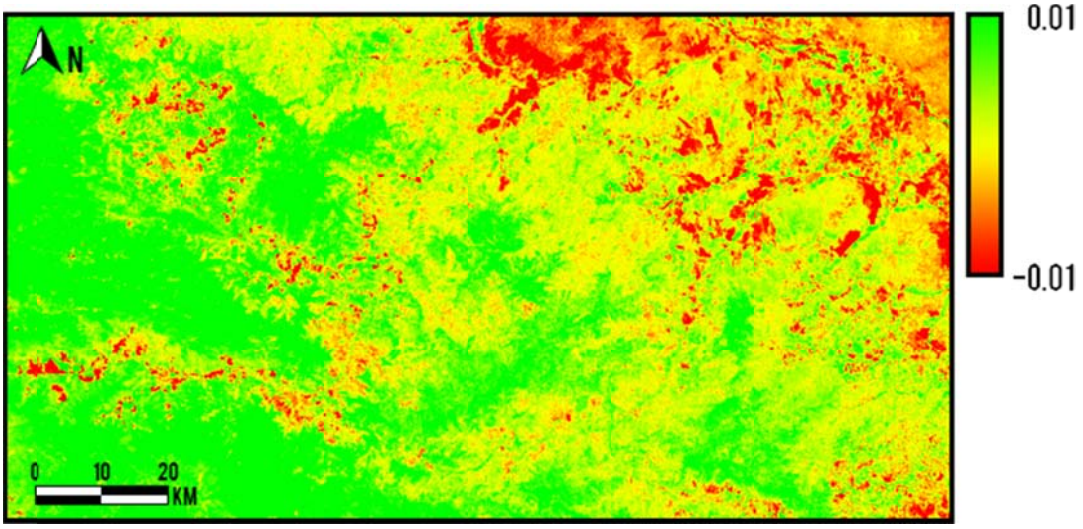

Figure 12: Long term trends of NDMI (using FormaTrend)

FormaTrend algorithm uses the time start property and it is used only to sort the collection, rather than populate the independent variable. As a result the calculated slopes are not correct for the collection with missing data. As the current dataset had big time gap (1988-1998), it was concluded that the method cannot be used for further analysis.

Afterwards, reducer was used that computes the slope and offset for a (weighted) linear regression of 2 inputs. LinearFit takes both x and y as input, which shows that the slope is correctly calculated in the dataset with missing data. The reducer takes the mask into account

as a weight. This indicates, that pixels that are only partially covered by region are weighted less in the fit.

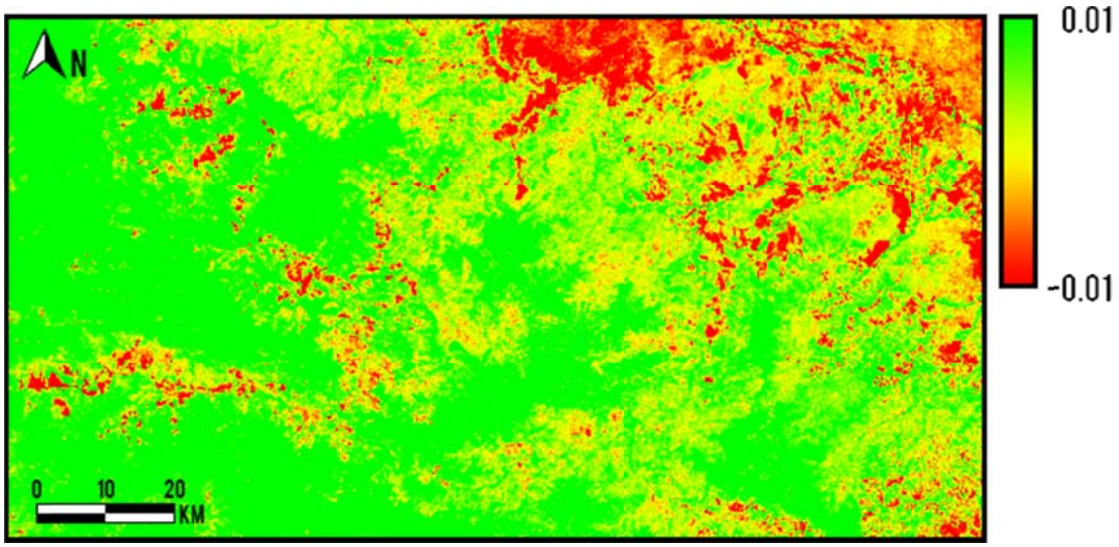

Figure 13: Long term trends of NDMI (Using linear reducer)

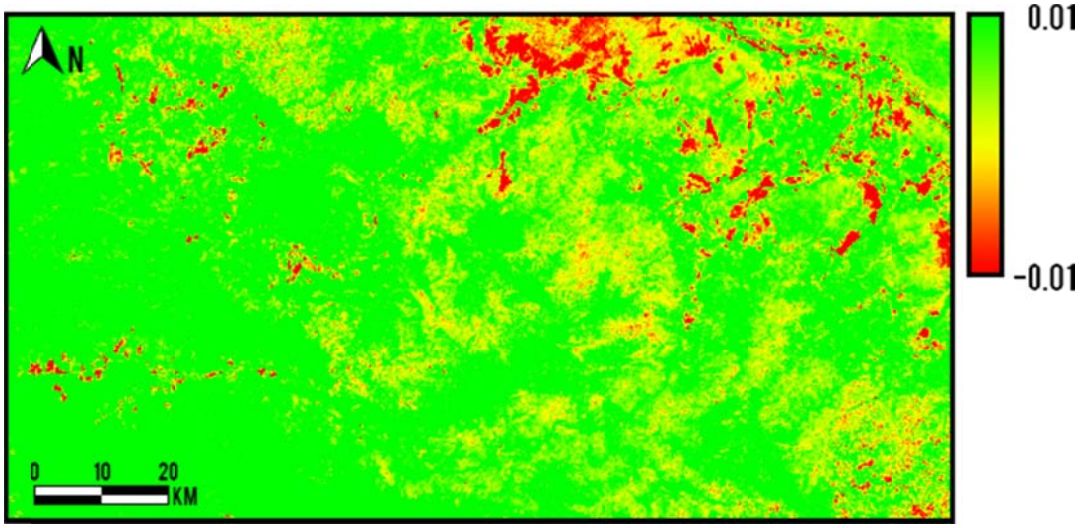

Figure 14: Long term trends of NDVI (Using linear reducer)

Figure 13 and 14 illustrate the results of trend analysis using linear reducer and display of linear slope. In order to compare these methods and to test the significance, the values of VIs were extracted, and the slope of the regression line was calculated outside GEE environment. In order to assess if the calculated trends are significant or not t-statistics and the residuals were reviewed. The areas with negative values of slope, which are considered as forest disturbances had low values of t-statistics, by which the disturbances were not considered as statistically significant.

5.2 Forest Masking and Within Forest Trend Analysis

The resulted trend maps had some misleading areas with forest disturbances, where the area is not covered by forest. Therefore, to have better accuracy of detection of trends in forest change, forest layer was generated. Similar approach was used by Hansen et al., (2013) to calculate the loss within the forest cover.

To achieve this aim, Hansen's tree cover layer was used to automatically generate the forest layer. The treecover2000 band of the UMD/hansen/global_forest_change_2013 image provides information about the tree cover around the globe in the year 2000 and its available in GEE (Google Earth Engine.API tutorial 2014).

In general the procedure of forest masking can be aggregated to following steps:

1. Train a classifier and obtain classified image
2. Extract a mask of forest cover
3. Map a function over the original reflectance image collection

Similar method was described by Huang et al., (2008), where training data were automatically generated using input satellite images and existing land cover products. The derived training data allow producing reliable forest cover products. The identified forest pixels then can be used as reference for delineating non-forest training samples.

Earth Engine supports the supervised classification of raster imagery. The process involves calling two methods: trainClassifier to build a classification model and classifyImage to apply the model. The training samples were obtained by sampling and 10000 points were randomly generated. Classification and Regression Tree (CART) was chosen as a classification method. The use of binary decision trees for classification is a nonparametric approach to pattern recognition. A decision tree provides a hierarchical representation of the feature space, in which patterns are allocated to classes according to the result obtained by following decisions made at a sequence of nodes at which branches of the tree diverge. CART letters indicate that trees may be used not only to classify entities into a discrete number of groups, but also as an alternative approach to regression analysis in which the value of a response (dependent) variable is to be estimated, given the value of each variable in a set of explanatory (independent) variables (Bittencourt & Clarke, 2003).

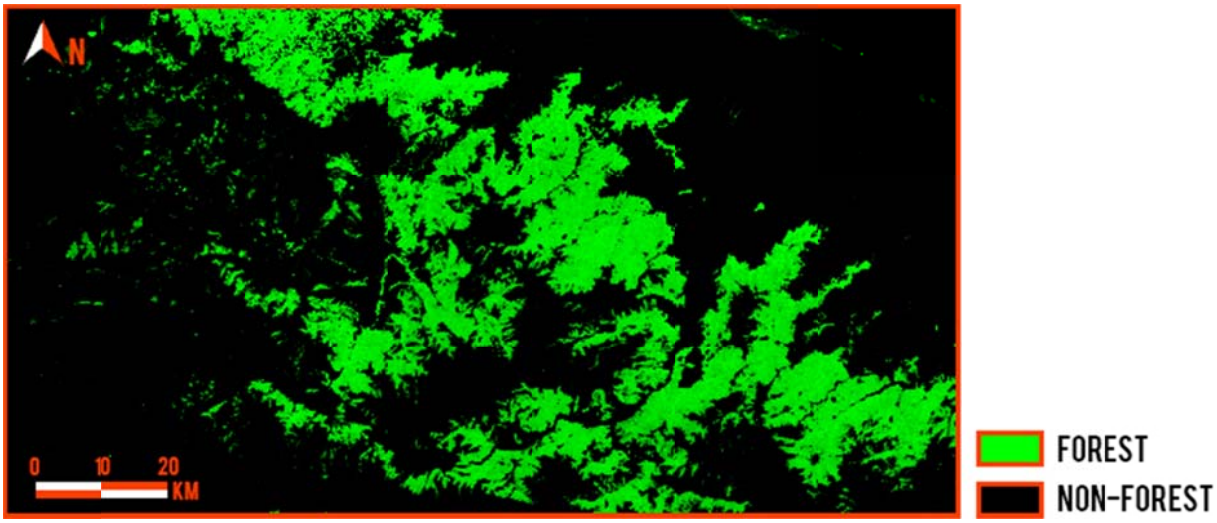

Figure 15: Generated forest cover layer

The resulted forest layer depicts the pixels which has forest cover more than 75% and covers around 2298 square km. This includes natural and planted forested areas. The area comprised by this tree cover layer is more than the area of officially registered forests as it includes areas covered by trees, which are not registered by state organizations.

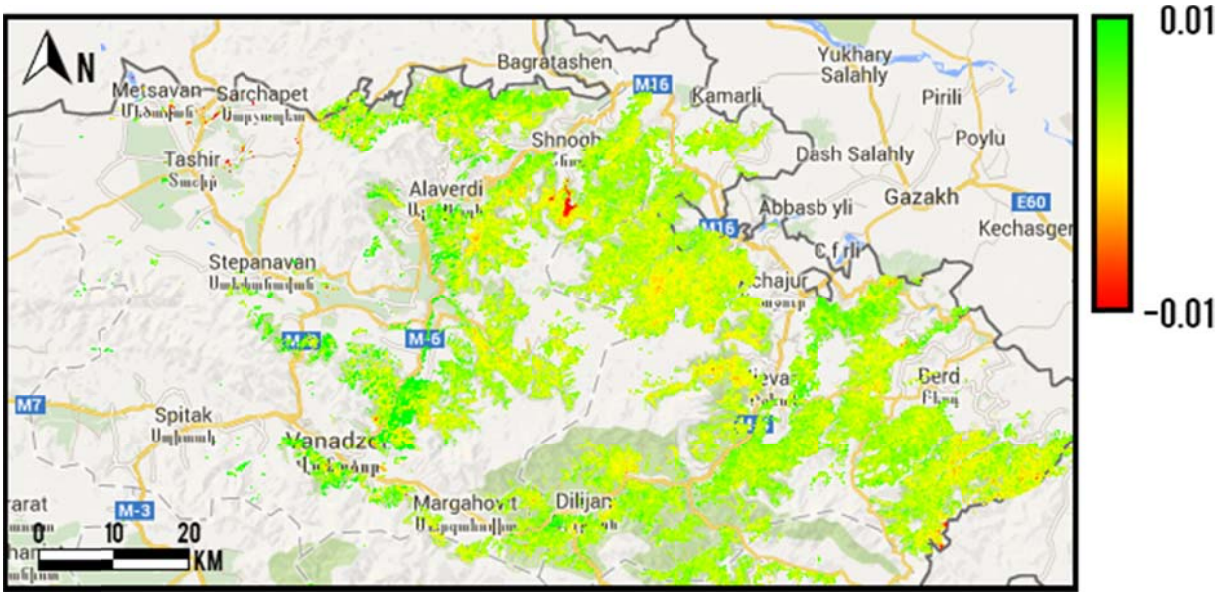

Figure 16: Forest trends estimated using NDVI

The next phase was the masking initial composites with resulted forest layer, which eliminates non forest areas. Afterwards the VI trends were estimated. Figure 16 and 17 show the trends after non-forest masking. The procedure of forest masking improved the results of analysis by eliminating the number of false negative trends.

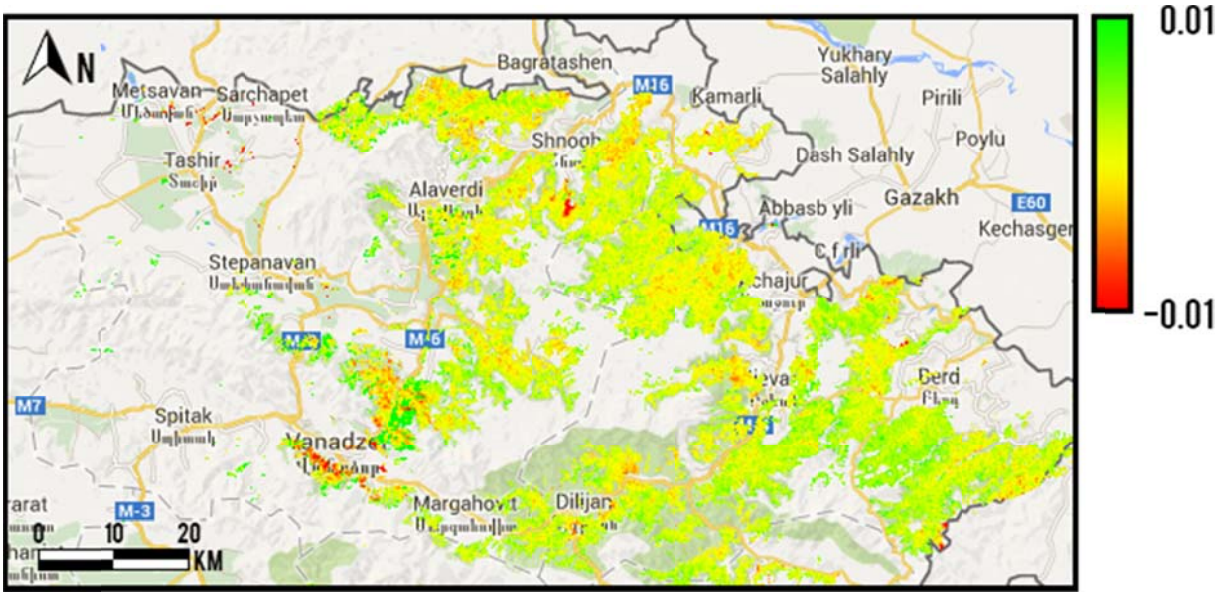

Figure 17: Forest trends estimated using NDMI

We assumed that areas with negative slope of the regression describe the forest disturbances. The following figures (Figure 18, 19) illustrate the resulted forest disturbance areas. As we can notice the areas with negative slopes were depicted more when using NDMI.

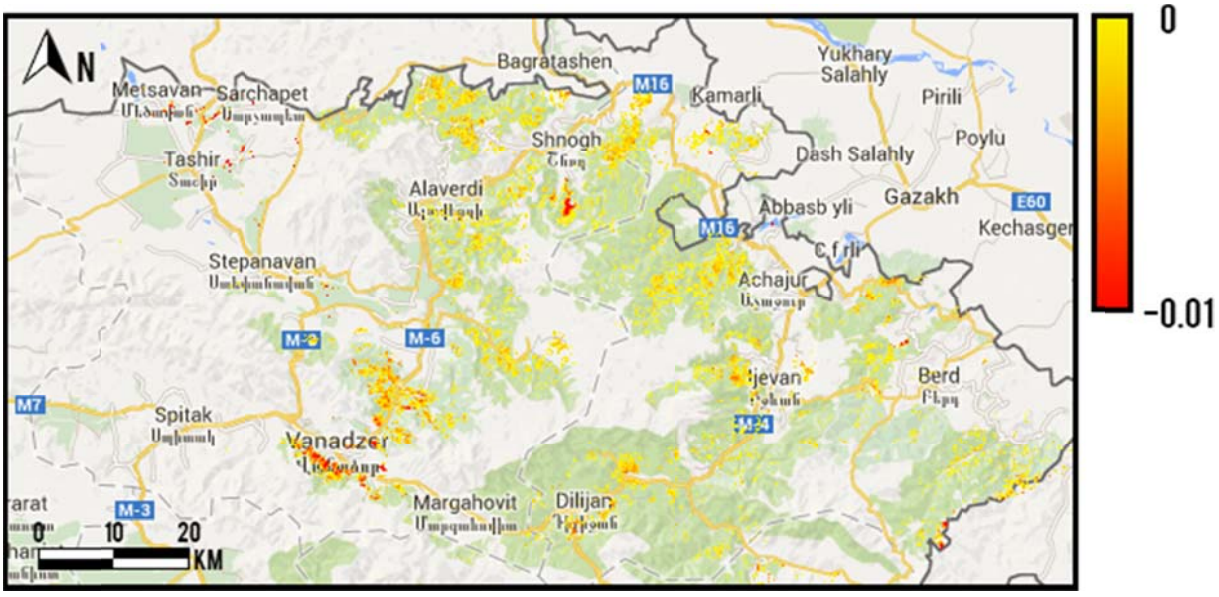

Figure 18: Negative NDMI trends (after non-forest masking)

Figure 19: Negative NDVI trends (after non-forest masking)

CHAPTER SIX
RESULTS AND DISSCUSSION

Trends in the forest area were derived using an ordinary least squares slope of the regression of vegetation index value versus time. Forest disturbances were not allocated annually, but over the entire study period derived from the negative slopes of regression analysis during leaf on season.

As a result it was found that in the period 1984-2014, the loss of forest reached about 7% (156 km^2) estimated by NDVI, and 22.9% (516 km^2) estimated by NDMI.

For checking the truthfulness of the results several validation techniques were used. It is described in the previous section that the trends were not significant in the areas of forest disturbance. This can be caused by the limited number of observations available during a long term and their sparse distribution over the time. Another reason can be the year-to-year variations in weather conditions on plant activity or ecosystem disturbances (Forkel et al., 2013).

To validate the forest disturbances, 21 polygons were used, which depict the partial harvests in the study area. In addition, the annual report of the State forest monitoring center of Armenia and the historical data of forest cover dynamics (Hengeryan et al., 2006; State forest monitoring center of Armenia, 2014) were made use of.

The resulted forest disturbance layers were clipped with ground truth polygons, and the number of polygons where there are forest loss pixels (presence/absence) was calculated.

Then simple ratio was made, which shows that NDVI had a 70% accuracy, while NDMI 95% accuracy. These results are in appliance with other studies (Wilson & Sader, 2002) and this outcome reports that the replacement of red band with SWIR significantly increases the accuracy of forest harvest detection. This can be due to the ability of SWIR to absorb water which leads to improvement of characterization of change especially in the early stages of forest harvests.

The spatial distributions of forest cover change during the time period shows specific locations of disturbances. They are mainly spotted near the cities and roads.

It is known, that aspects can have a strong influence on vegetation as the south facing slopes are generally drier than the north facing slopes. For this purpose terrain was studied and aspect values were calculated. As the forest disturbances were depicted in both north facing and south facing slopes, we concluded that the results are not affected by terrain.

Temporal variability of VI change was also studied. At the locations, where negative slopes were depicted, the VI values were plotted against time. Figure 20 illustrates the results, from which we can notice that there is a pattern in decline in 1999. This is logical, as the forests were under the highest anthropogenic pressure during the 1990s. 191 km^2 forest loss was depicted during the 1987-2000 (Sayadyan 2007, Thuresson et al., 1999, based on national inventory data). Another estimate of forest loss 1993-2000 is around 540km^2 (Hengeryan et al., 2007). The estimates are different, but they clearly show that there was a dramatic loss of forest during the 1990s and the decline in 1999 is justified.

Furthermore, in most of the locations, there was a decline in 2003-2004 which can be justified by the large amount of wind-blown trees during those years. In addition, the official forest logging data published by Hayantar (2014) also depict these years with the high amount of cuts.

Also the annual report of the State forest monitoring center of Armenia was studied, and the depicted decline from 2010 coincides with the peak of illegal logging starting from 2009. They justify the increasing pressure on the forest by the rise of the price of electricity and gas in recent years.

Overall, from the analysis of the trajectories, the values of coefficients we can see that there is no major increasing or decreasing trend and the values of vegetation indices fluctuate over time. This brings an assumption that after the decrease there was reforestation and trees grow back after the disturbance. To back this assumption, differences of the composites from the start and the end of time period were calculated. The smaller values of these differences than those of the depicted disturbance values endorse the discussed assumption.

Although we can see that GEE provides functionalities for advanced analysis, there were some limitations that we encountered. Because of the limitation of the used reducer (limited number of pixels), we were not able to run calculations with the original resolution. Another concern was the significance of the estimated trends. This is of primary importance since it demonstrates the accuracy of our analysis.

Despite the facts that the trends of the individual pixels are not significant, the trends can be more significant from spatially averaged coefficients. Because of the time restrictions, we were not able to develop the algorithms but it can be considered in further research.

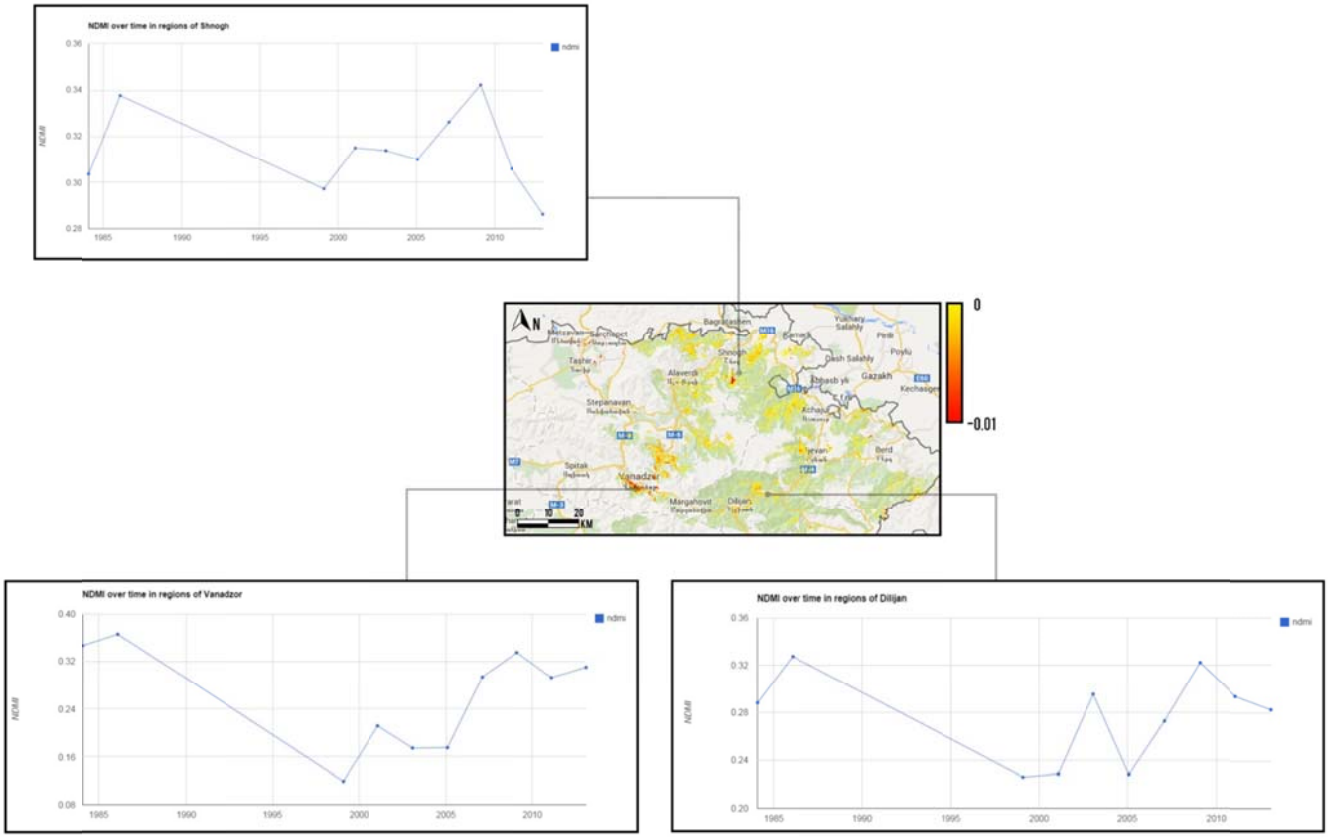

Figure 20: Trajectories of NDMI value over a regions of negative trends

CONCLUSIONS AND RECOMMENDATIONS

The results that we got from the study greatly influenced on our conclusions and helped to answer to all research questions.

Research question 1

Is it possible to detect patterns and trends of forest changes in local scale using temporally dense Landsat collections? How scientifically robust is the use of those data to identify the changes in the study area taking into account the limitations of study?

From the results that were obtained it can be concluded that the available Landsat collections can provide sufficient information for identifying forest changes. It should be mentioned, that Landsat images are highly affected by clouds and missing scan lines due to the failure of scan line corrector in 2003. As a result careful preprocessing should be carried out. Although the data were not enough for analyzing the changes with annual composites, biannual composites were created.

Research question 2

What kind of techniques could be used to analyze forest cover change? Are those methods relevant for research in local scale?

Considering the limitations of data availability, 10 epochal composites were generated, which is practically an adequate number for trend analysis. The creation of continuous composites was possible due to the use of pixel based compositing method.

Time series of vegetation indices were used. Two VI were chosen: NDVI and NDMI. Afterwards pixel based ordinary least squares regression was performed where dependent variable y was the value of VI. As a result the areas with negative slopes of regression were defined as forest disturbance. To eliminate overestimation in the non-forest areas, the forest cover layer was generated. The original composites were masked and as a result the changes in forest areas were obtained. Afterwards the results were compared with ground truth data. This proves that time series of VI enable detection and quantification of gradual changes within the time frame covered. Both of the VIs used in the study were effective for detecting clear cuts. NDMI was more sensitive for partial harvests.

From the results we can conclude that the methods are relevant and provide favorable evidence of forest disturbances. GEE provides open access to satellite imagery and makes easier the use of above mentioned methods and extraction of interpretable results.

Research question 3

What is the trend of forest cover change in the study area?

The results show that in 23% of forest area there were negative trends during the study period. The main areas of forest disturbances are close to populated areas and roads.

The causes of the disturbances can be different. The main reasons are human-modification of the forest for industrial and (e.g. large clear cuts in Shnogh area) household (partial cuts around the cities) use. In addition, the forest was affected by natural disasters (wind, landslides).

Future research needs more sophisticated algorithms for evaluating the significance of trends. Furthermore, the effects of weather related fluctuations of forest ecosystem must be taken into consideration in a great detail.

BIBLIOGRAPHY

Almutairi, A., & Warner, T. A. (2010). Change detection accuracy and image properties: a study using simulated data. Remote Sensing, 2(6), 1508-1529.

Asryan A. (2005) Deforestation – View from the Space, project funded by Rudolf foundation

Bhandari, S., Phinn, S., & Gill, T. (2012). Preparing Landsat Image Time Series (LITS) for monitoring changes in vegetation phenology in Queensland, Australia. *Remote Sensing*, *4*(6), 1856-1886.

Bittencourt, H. R., & Clarke, R. T. (2003, July). Use of classification and regression trees (CART) to classify remotely-sensed digital images.*Geoscience and Remote Sensing Symposium, 2003. IGARSS'03. Proceedings. 2003 IEEE International* (Vol. 6, pp. 3751-3753). IEEE.

Cohen, W. B., & Goward, S. N. (2004). Landsat's role in ecological applications of remote sensing. *Bioscience*, *54*(6), 535-545.

Cohen, W. B., Yang, Z., & Kennedy, R. (2010). Detecting trends in forest disturbance and recovery using yearly Landsat time series: 2. TimeSync—Tools for calibration and validation. *Remote Sensing of Environment*, *114*(12), 2911-2924.

D. Lu, Q. Weng (2007), A survey of image classification methods and techniques for improving classification performance, International Journal of Remote Sensing, , Vol. 28, No. 5, pp.823-870.

FAO (Food and Agriculture Organization of the United Nations). (2007). Manual on Deforestation, Degradation and Fragmentation Using Remote Sensing and GIS.Working Paper 5: FAO; Rome.

FAO (Food and Agriculture Organization of the United Nations). (2010). *Global Forest Resources Assessment 2010 Main Report*. FAO.

Forkel, M., Carvalhais, N., Verbesselt, J., Mahecha, M. D., Neigh, C. S., & Reichstein, M. (2013). Trend change detection in NDVI time series: Effects of inter-annual variability and methodology. *Remote Sensing*, *5*(5), 2113-2144.

Griffiths, P., Kuemmerle, T., Kennedy, R. E., Abrudan, I. V., Knorn, J., & Hostert, P. (2012). Using annual time-series of Landsat images to assess the effects of forest restitution in post-socialist Romania. *Remote Sensing of Environment*, *118*, 199-214.

Hansen, M. C., P. V. Potapov, R. Moore, M. Hancher, S. A. Turubanova, A. Tyukavina, D. Thau, S. V. Stehman, S. J. Goetz, T. R. Loveland, A. Kommareddy, A. Egorov, L. Chini, C.

O. Justice, and J. R. G. Townshend. 2013. "High-Resolution Global Maps of 21st-Century Forest Cover Change." Science 342 (15 November): 850–53, available on-line at: http://earthenginepartners.appspot.com/science-2013-global-forest.

Hais, M., Jonášová, M., Langhammer, J., & Kučera, T. (2009). Comparison of two types of forest disturbance using multitemporal Landsat TM/ETM+ imagery and field vegetation data. *Remote Sensing of Environment*, *113*(4), 835-845.

Hayes, D. J., & Cohen, W. B. (2007). Spatial, spectral and temporal patterns of tropical forest cover change as observed with multiple scales of optical satellite data. *Remote Sensing of Environment*, *106*(1), 1-16.

Hergnyan, M.,Hovhannisyan, S., Grigoryan, S., & Sayadyan, H. (2006). The economics of Armenia's forest industry. *The economics of Armenia's forest industry.*

Hirschmugl, M., Steinegger, M., Gallaun, H., & Schardt, M. (2014). Mapping Forest Degradation due to Selective Logging by Means of Time Series Analysis: Case Studies in Central Africa. *Remote Sensing*, *6*(1), 756-775.

Huang, C., Song, K., Kim, S., Townshend, J. R., Davis, P., Masek, J. G., & Goward, S. N. (2008). Use of a dark object concept and support vector machines to automate forest cover change analysis. *Remote Sensing of Environment*, *112*(3), 970-985.

Jianya, G., Haigang, S., Guorui, M., & Qiming, Z. (2008). A review of multi-temporal remote sensing data change detection algorithms. *The International Archives of the Photogrammetry, Remote Sensing and Spatial Information Sciences*, *37*(B7), 757-762.

Jin, S., & Sader, S. A. (2005). Comparison of time series tasseled cap wetness and the normalized difference moisture index in detecting forest disturbances. *Remote sensing of Environment*, *94*(3), 364-372.

Jong, R. D., & Bruin, S. D. (2012). Linear trends in seasonal vegetation time series and the modifiable temporal unit problem. *Biogeosciences*, *9*(1), 71-77.

Junge, N., Fripp, E. (2011).Understanding the forestry sector of Armenia: Current conditions and choices.

Lehmann, E. A., Wallace, J. F., Caccetta, P. A., Furby, S. L., & Zdunic, K. (2013). Forest cover trends from time series Landsat data for the Australian continent. *International Journal of Applied Earth Observation and Geoinformation*, *21*, 453-462.

Moreno-Sanchez, R., & Sayadyan, H. Y. (2005). Evolution of the forest cover in Armenia. *International Forestry Review*, *7*(2), 113-127.

Moreno-Sanchez, R., Sayadyan, H., Streeter, R., Rozelle, J., Tiezzi, E., Marques, J. C., & Jørgensen, S. E. (2007). The Armenian forests: threats to conservation and needs for sustainable management. In *Sixth International Conference on Ecosystems and Sustainable Development, Coimbra, Portugal, September 2007.* (pp. 113-122). WIT Press.

Reiche J., Verbesselt J. , Herold M., Lagataki S., Lewai A. (2013). Landsat and (SAR) time-series for detecting forest change in Fiji at high temporal resolution.

Rogan, J., Miller, J., Wulder, M. A., & Franklin, S. E. (2006). Integrating GIS and remotely sensed data for mapping forest disturbance and change. *Understanding forest disturbance and spatial pattern: remote sensing and GIS approaches*, 133-172.

Sayadyan, H. Y., & Moreno-Sanchez, R. (2006). Forest policies, management and conservation in Soviet (1920–1991) and post-Soviet (1991–2005) Armenia.*Environmental Conservation*, *33*(01), 60-72.

Sayadyan, H. 2007. Non-regulated and illegal logging in Armenia and its consequences. *Bulletin of State Agrarian University of Armenia*, N1, Yerevan, P.23-27.

Thomas, N. E., Huang, C., Goward, S. N., Powell, S., Rishmawi, K., Schleeweis, K., & Hinds, A. (2011). Validation of North American forest disturbance dynamics derived from Landsat time series stacks. *Remote Sensing of Environment*, *115*(1), 19-32.

Thuresson, T., Drakenberg, B., & Ter-Ghazaryan, K. (1999). Forest Resources Assessment for Armenia, SIDA-Armenia project (1997-1999). *Yerevan, Armenia: Ministry of Nature Protection*.

Verbesselt, J., Hyndman, R., Newnham, G., & Culvenor, D. (2010). Detecting trend and seasonal changes in satellite image time series. *Remote sensing of Environment*, *114*(1), 106-115.

Verbesselt, J., Zeileis, A., & Herold, M. (2012). Near real-time disturbance detection using satellite image time series. *Remote Sensing of Environment*, *123*, 98-108.

Vogelmann, J. E., Xian, G., Homer, C., & Tolk, B. (2012). Monitoring gradual ecosystem change using Landsat time series analyses: case studies in selected forest and rangeland ecosystems. *Remote Sensing of Environment*, *122*, 92-105.

Weng, Q. (Ed.). (2011). *Advances in environmental remote sensing: sensors, algorithms, and applications*. CRC Press.

Wilson, E. H., & Sader, S. A. (2002). Detection of forest harvest type using multiple dates of Landsat TM imagery. *Remote Sensing of Environment*, *80*(3), 385-396.

White, J. C., Wulder, M. A., Hobart, G. W., Luther, J. E., Hermosilla, T., Griffiths, P., Guindon, L. (2014). Pixel-based image compositing for large-area dense time series applications and science. *Canadian Journal of Remote Sensing*, *40*(3), 192-212.

Wulder, M. A., White, J. C., Masek, J. G., Dwyer, J., & Roy, D. P. (2011). Continuity of Landsat observations: Short term considerations. *Remote Sensing of Environment*, *115*(2), 747-751.

Armenian Tree Project (2013).The problem and current situation, available at: http://www.armeniatree.org/ (Last accessed: 22.Jan.2015)

Global Forest Watch, Armenia, Available online at: http://www.globalforestwatch.org/country/ARM (Last accessed: 22.Jan.2015)

Google Earth Engine. API tutorial (2014), Available online at: https://sites.google.com/site/earthengineapidocs/tutorials/api-tutorial-introduction-to-the-earth-engine-api. (Last accessed: 25.Feb.2015)

Hayantar SNCO of the Ministry of Agriculture of the Republic of Armenia, available at: http://www.hayantar.am/en. (Last accessed: 22.Jan.2015)

Landsat missions (2014), U.S. Geological Survey, available online at: http://landsat.usgs.gov (Last accessed: 22.Jan.2015)

State forest monitoring center of Armenia, available at: http://www.forest-monitoring.am/ (Last accessed: 25.Feb.2015)

ATTACHMENTS

GEE script

The code is available also online and it can be accessed and executed with the following link: https://ee-api.appspot.com/3a8184d8249b671b855c52677a750da2

```
// Analysis of spatial and temporal variations of forest
// A case of study in northeastern Armenia
// Gohar Ghazaryan
// Master of Science in Geospatial Technologies


//-----------------------------------------Defining the extend of study area----------------------------------//

var aoi= ee.FeatureCollection(ee.Feature(ee.Geometry.Rectangle(44, 40.65, 45.6, 41.3)));
var aoigeometry =ee.Geometry.Rectangle(44, 40.65, 45.6, 41.3);
Map.setCenter(44.7, 40.8, 10);
addToMap(ee.Image().paint(aoi,1,1),{},'Study_Area');


//-----------------------------------------simpleCloudScore function-----------------------------------------//
var cloud_thresh = 20;
var shadowSumBands = ['nir','swir1','swir2'];
var cloud_filter = function(image) {
  image = ee.Algorithms.Landsat.simpleCloudScore(image);
  var quality = image.select('cloud').gt(cloud_thresh);

  var maskedImage = image.mask().and(quality.not());
  image = image.mask(maskedImage);
  return image;
};

var maskIncomplete = function(image)
  {
    var incompleteThreshold = -0.001;
    var imageWhere = image.where(
      image.select([0]).gte(incompleteThreshold)
    .and(image.select([1]).gte(incompleteThreshold))
    .and(image.select([2]).gte(incompleteThreshold))
    .and(image.select([3]).gte(incompleteThreshold))
    .and(image.select([4]).gte(incompleteThreshold))
    .and(image.select([5]).gte(incompleteThreshold))
    .and(image.select([6]).gte(incompleteThreshold)),10);

    return image.mask(image.mask().and(imageWhere.select([1]).eq(10)));
  };

var addIndices = function(in_image){

    in_image = in_image.select([0,1,2,3,4,5,6],STD_NAMES);
    in_image = in_image.addBands(in_image.normalizedDifference(['nir',
'red']).select([0],['ndvi']).toFloat());
    in_image = in_image.addBands(in_image.normalizedDifference(['nir',
'swir1']).select([0],['ndmi']).toFloat());
```

```
    return in_image;

};

//----------------------------------------Adding a time band-------------------------------------------------//

var set_date_time = function(in_image, year1,year2){

//Set some time properties
  var time_start = new Date(year1,6,1);
  var time_end = new Date(year2,9,1);
  in_image = in_image.set({
     'system:time_start': time_start.valueOf(),
     'system:time_end': time_end.valueOf(),
     'system:year_start': year1,
     'system:year_end':year2
  });
  return in_image;
  };

var MSEC_PER_TIMESTEP = 60*365*2*60*24*1000;
var addDateBand = function(inImg){
  var i =inImg.metadata('system:time_start').divide(MSEC_PER_TIMESTEP).toFloat();
  return inImg.addBands(ee.Image(i).select([0], ['Date']));

};

//----------------------------------------Getting the data for forest layer prediction----------------------//

// Specifying temporal window
var start_day = 182;// July 1
var end_day = 274;// October 1
var shadowSumThresh = 0.3;

//  A mapping from a common name to the sensor-specific bands
var STD_NAMES = ['blue', 'green', 'red', 'nir', 'swir1', 'temp','swir2'];
var vizParamsCO = {'min': 0.05,'max': [.3,0.4,.4],   'bands':'swir1,nir,red'};
var vizParamsHansenTC = {'min':20, 'max':100, 'palette': '000000, 00FF00'};

var getImage = function(years){
  var year1 = years[0];
  var year2 = years[1];
  var iEnd =year1.toString() + '_'+year2.toString();
  var img = ee.ImageCollection('L5_L1T_TOA')
          .filterDate(new Date('1/1/'+year1.toString()),new
Date('12/31/'+year2.toString()))
          .filter(ee.Filter.calendarRange(start_day,end_day))
          .filterBounds(aoigeometry)
          .map(function(img){
            var  filtered = cloud_filter(img).select([0,1,2,3,4,5,6],STD_NAMES);
             filtered = maskIncomplete( filtered);
            var sum =  filtered.select(shadowSumBands).reduce(ee.Reducer.sum());
            filtered =  filtered.mask( filtered.mask().and(sum.gt(0.3)));
            return  filtered});
  img =img.reduce(ee.Reducer.percentile([50])).select([0,1,2,3,4,5,6],STD_NAMES);
  img = addIndices(img);
  img = set_date_time(img,year1,year2);
  //addToMap(img.clip(aoigeometry),vizParamsCO,'img_'+iEnd,false);
```

```
  return img;
};

var sampleNumber = 10000;
var modelYears = [2000,2012];
var applyYearList = [[1984,1990]];
var mode ='regression';

// A region of the image to train with
var trainingPolygon = ee.FeatureCollection(ee.Feature(ee.Geometry.Rectangle(44.3, 40.6,
45.5, 41.2)));
var points = ee.FeatureCollection.randomPoints(trainingPolygon, sampleNumber, 1, 1);

//Adding data
var hansenFC =
ee.Image('UMD/hansen/global_forest_change_2013').select('treecover2000');
var cover = hansenFC;
var vizParamsCover = vizParamsHansenTC;
//addToMap(cover, vizParamsCover, 'Calibration Raster');

var terrain = ee.Algorithms.Terrain('CGIAR/SRTM90_V4');
var modelData = cover.addBands(getImage(modelYears).addBands(terrain));
var applyData = getImage([1984,1985]).addBands(terrain);
var applyImages  = applyYearList.map(function(yr){return
getImage(yr,start_day,end_day,shadowSumThresh).addBands(terrain)});

//Get the band names
var bandNames =modelData.bandNames();
var trainingName = bandNames;
var predictorNames = bandNames.slice(1,bandNames.length-1);

// Training the classifier with specified inputs
var trainModel = function(points,modelData,trainingName,predictorNames,
classificationMode){

  var training = modelData.reduceToVectors({
    reducer: "mean",
    geometry: points,
    geometryType: "centroid",
    scale: 30,
    tileScale: 7,
    crs: "EPSG:4326"})
    .filter(ee.Filter().neq('blue', null))
    .filter(ee.Filter().neq('elevation', null))
    .filter(ee.Filter().neq('slope', null));
  //addToMap(training,{},'training',false);

  var classifier = training.trainClassifier({
    property_list: predictorNames,
    class_property: 'label',
    classifier_mode: classificationMode,
    classifier_name: "Cart"});
  return classifier;
};

var applyModel = function(model,applyData,predictorNames){
  // Apply the classifier to the original composite.
  var output = applyData.select(predictorNames).classify(model);
```

```
  //addToMap(output.clip(aoigeometry), vizParamsCover,'forest');
  return output;
};

var model = trainModel(points,modelData,trainingName,predictorNames,mode);
var forest_cover = applyImages.map(function(applyData){return
applyModel(model,applyData,predictorNames)});

//--------------------------------Trend analysis ------------------------------------------------------------------//
// Years for creating the composites

 var years =
[[1984,1985],[1986,1987],[1999,2000],[2001,2002],[2003,2004],[2005,2006],[2007
,2008],[2009,2010],[2011,2012],[2013,2014]];


var getImage = function(years,start_day,end_day,shadowSumThresh){
  var year1 = years[0];
  var year2 = years[1];
  var iEnd =year1.toString() + '_'+year2.toString();

  var img = ee.ImageCollection('LANDSAT/LT5_L1T_TOA')
          .filterDate(new Date('7/1/'+year1.toString()),new Date('10/1/'+year2.toString()))
          .filter(ee.Filter.calendarRange(start_day,end_day))
          .filterBounds(aoi)
          .map(function(img){
            var filtered = cloud_filter(img).select([0,1,2,3,4,5,6],STD_NAMES);
            filtered = maskIncomplete(filtered);
            var sum = filtered.select(shadowSumBands).reduce(ee.Reducer.sum());
            filtered = filtered.mask(filtered.mask().and(sum.gt(shadowSumThresh)));
            return filtered;
          });
  var img2 = ee.ImageCollection('LANDSAT/LE7_L1T_TOA')
          .filterDate(new Date('7/1/'+year1.toString()),new Date('10/1/'+year2.toString()))
          .filter(ee.Filter.calendarRange(start_day,end_day))
          .filterBounds(aoi)
          .map(function(img){
            var filtered = cloud_filter(img).select([0,1,2,3,4,5,7],STD_NAMES);
            filtered = maskIncomplete(filtered);
            var sum = filtered.select(shadowSumBands).reduce(ee.Reducer.sum());
            filtered = filtered.mask(filtered.mask().and(sum.gt(shadowSumThresh)));
            return filtered;
          });
  img = ee.ImageCollection(img.merge(img2));
  img =img.reduce(ee.Reducer.percentile([50])).select([0,1,2,3,4,5,6],STD_NAMES);
  img = img.clip(aoi);
  img = img.mask(forest_cover[0].gt(75));
  img = addIndices(img);
  img = set_date_time(img,year1,year2);
//addToMap(img.clip(aoigeometry),vizParamsCO,'img_'+iEnd,false);
  return img;
};
 var images = ee.ImageCollection(years.map(function(yr){return
getImage(yr,start_day,end_day,shadowSumThresh)}));
var images = images.map(addDateBand);
print(images);
```

```
// Adding the polygon of Armenia
var countries = ee.FeatureCollection('ft:1tdSwUL7MVpOauSgRzqVTOwdfy17KDbw-
1d9omPw');
var Armenia = countries.filterMetadata('Country', 'equals', 'Armenia');

// Extracting the series of  VI

var ndvis = images.select(['ndvi']);
var ndmis = images.select(['ndmi']);

// Individual differences of composites from the start and the end of time period
var ndvi1984 = ndvis.filterDate(
  '1984-01-01', '1999-12-31').median();

var ndvi2014 = ndvis.filterDate(
  '2009-01-01', '2014-12-31').median();
  var difference = ndvi2014.subtract(ndvi1984);
//addToMap(difference.clip(aoigeometry),
 // {'palette':'FF0000, 000000, 00FF00',
//   'min': -0.15, 'max': 0.15
//  });
 var differenceLoss= difference.mask(difference.lt(0)).clip(aoigeometry).clip(Armenia);
 //addToMap(differenceLoss.clip(aoigeometry),
//  {'palette':'FF0000',
//   'min': -0.15, 'max': 0
//  });

 var num_differenceLoss=differenceLoss.reduceRegion(ee.Reducer.count(), aoi,250);
print(num_differenceLoss,'NDVI difference');

var ndmi1984 = ndmis.filterDate(
  '1984-01-01', '1999-12-31').median();

var ndmi2014 = ndmis.filterDate(
  '2009-01-01', '2014-12-31').median();

var differenceNDMI = ndmi2014.subtract(ndmi1984);
//addToMap(differenceNDMI.clip(aoigeometry),
 // {'palette':'FF0000, 000000, 00FF00',
 //   'min': -0.15, 'max': 0.15
 // });
var differenceLossNDMI=
differenceNDMI.mask(differenceNDMI.lt(0)).clip(aoigeometry).clip(Armenia);
// addToMap(differenceLossNDMI.clip(aoigeometry),
 // {'palette':'FF0000',
 //   'min': -0.15, 'max': 0
 // });

 var num_differenceLossNDMI=differenceLossNDMI.reduceRegion(ee.Reducer.count(), aoi,250);
print(num_differenceLossNDMI,'NDMI difference');


//----------------------------------------Forma trend ndvi----------------------------------------------//
var trends = ndvis.formaTrend();
var ltTrend = trends.select(['long-trend']).clip(Armenia).clip(aoigeometry);
//addToMap(ltTrend.mask(ltTrend.lt(0.1).clip(aoigeometry)), { min: -0.01, max: 0.01,'palette':
'FF0000,FFFF00,00FF00'}, 'FormaTrend-Long term trend');
//----------------------------------------Forma trend ndmi----------------------------------------------//
var trends_ndmi = ndmis.formaTrend();
```

```
var ltTrend_ndmi = trends_ndmi.select(['long-trend']).clip(Armenia);

//addToMap(ltTrend_ndmi.mask(ltTrend.lt(0.1).clip(aoigeometry)), { min: -0.01, max: 0.01,'palette':
'FF0000,FFFF00,00FF00'}, 'FormaTrend_ndmi');


//----------------------------------------Linear fit reducer for ndvi----------------------------------------//
var linearFit_ndvi =
images.select(['Date','ndvi']).reduce(ee.Reducer.linearFit()).clip(Armenia);
var linearFit_ndvi = linearFit_ndvi.select(['scale']);
//addToMap(linearFit_ndvi.clip(aoigeometry),{ min: -0.01, max: 0.01,'palette':
'FF0000,FFFF00,00FF00'}, 'linearFitReducer_ndvi');
var loss_ndvi= linearFit_ndvi.mask(linearFit_ndvi.lt(0)); // masking the values
//addToMap(loss_ndvi.clip(aoigeometry).clip(Armenia), { min: -0.01, max: 0,'palette':
'FF0000,FFFF00'}, 'loss_linearfit_ndvi');

var num_loss_ndvi=loss_ndvi.reduceRegion(ee.Reducer.count(), aoi, 250);
print(num_loss_ndvi, 'NDVI loss');


//----------------------------------------Linear fit reducer for ndmi----------------------------------------//

var linearFit_ndmi =
images.select(['Date','ndmi']).reduce(ee.Reducer.linearFit()).clip(Armenia);
var linearFit_ndmi = linearFit_ndmi.select(['scale']);
addToMap(linearFit_ndmi.clip(aoigeometry),{ min: -0.01, max: 0.01,'palette':
'FF0000,FFFF00,00FF00'}, 'linearFitReducer_ndmi');
var loss_ndmi= linearFit_ndmi.mask(linearFit_ndmi.lt(0)); // masking the values
addToMap(loss_ndmi.clip(aoigeometry).clip(Armenia), { min: -0.01, max: 0,'palette':
'FF0000,FFFF00'}, 'loss_linearfit_ndmi');
var num_loss_ndmi=loss_ndmi.reduceRegion(ee.Reducer.count(), aoi, 250);
print(num_loss_ndmi,'NDMI loss');

//----------------------------------------Temporal analysis----------------------------------------//
// Temporal trajectories of VI
// For other sites change the polygon to
// (44.82, 41.05, 44.87, 41.1) Shnogh
// (44.48, 40.785, 44.5, 40.8) Vanadzor
// (44.84, 40.7, 44.86, 40.73) Dilijan

var subsetShnogh =ee.Geometry.Rectangle(44.82, 41.05, 44.87, 41.1);
addToMap(subsetShnogh,'Shnogh');

//Chart series
var TimeSeries =
    Chart.image.series(ndmis,subsetShnogh, ee.Reducer.mean(),200);
     TimeSeries = TimeSeries.setOptions({
  title: 'NDMI over time in regions of Shnogh',
  vAxis: {
    title: 'NDMI'
    },
  lineWidth: 1,
  pointSize: 4,
});
print(TimeSeries);
```